Development of a Benzimidazole-Based Protransporter with Photoactivatable Nitrate Transport Activity

A thesis

submitted to

Indian Institute of Science Education and Research Pune

in partial fulfillment of the requirements for the

BS-MS Dual Degree Programme

by

Anurag Singh

IISER PUNE

Indian Institute of Science Education and Research Pune

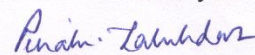**Dr. Homi Bhabha Road, Pashan, Pune 411008, INDIA**

April 2019

Supervisor: Dr. Pinaki Talukdar

Certificate

This is to certify that this dissertation entitled "**Development of benzimidazole-based protransporters with photocleavable anion transport activity**" towards the partial fulfilment of the BS-MS dual degree programme at the Indian Institute of Science Education and Research, Pune represents work carried out by **Anurag Singh** at Indian Institute of Science Education and Research under the supervision of **Dr. Pinaki Talukdar**, Associate Professor, Department of Chemistry, during the academic year 2018-2019.

Dr. Pinaki Talukdar

Committee:

Name of your Guide: Dr. Pinaki Talukdar

Name of Your TAC Member: Prof. M. Jayakannan

Declaration

I hereby declare that the matter embodied in the report entitled "**Development of benzimidazole-based protransporters with photocleavable anion transport activity**"are the results of the work carried out by me at the Department of Chemistry, Indian Institute of Science Education and Research, Pune, under the supervision of Dr. Pinaki Talukdar and the same has not been submitted elsewhere for any other degree.

Anurag

Mr. Anurag Singh

This Thesis is Dedicated to My Beloved Parents……..

Acknowledgments

Abstract

A very few synthetic transporters for nitrate ion have been reported till date. Nitrate transporters have found implication in gastric protection, platelet aggregation inhibition and blood pressure regulation along with nitrate transport in plants. Herein we report a transporter selectively transporting nitrate. These transporters mimic the work of natural nitrate transporter proteins along with spatiotemporal control for the transport attributed to the photocleavable group present in the transporter.

Contents

Table of figures

1. Introduction

1.1. Transport across cell membrane

Cells are the basic units of life. The cell membrane is composed of self-assembled lipid molecules, which contain the polar head groups facing the extracellular and intracellular aqueous environment. However, the internal part of the membrane is hydrophobic, hence impermeable to the polar solute molecules like amino acids, sugars, and ions. Membrane-embedded proteins that form channels, carriers or pumps, facilitate the transport of ions across the membrane. The process is essential for the survival of the cell as it regulates cellular pH, osmotic balance, cell volume, and signal transduction. Natural ion channels span the lipid bilayer and allow ions to pass through their transmembrane polar pores. While ion carriers, on the other hand, shuttle across the lipid bilayer membrane to transport ions.[1] In general, natural ion channels contain hydrophobic amino acid residues on the inner surface of the channel to allow ions to pass through it and hydrophobic amino acid residues on the outer surface to span the lipid bilayer. Ion carriers provide ion-binding sites that are orchestrated by polar residues of the proteins.
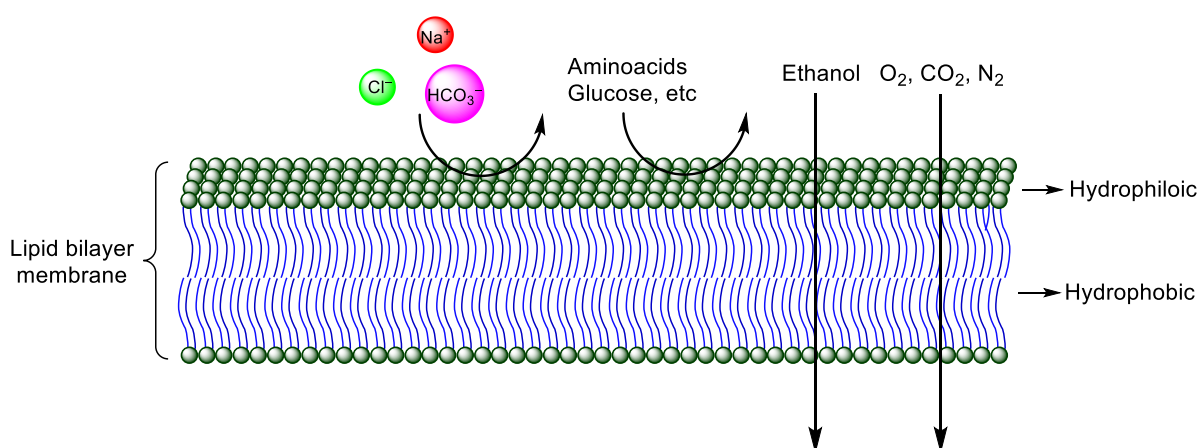
Figure 1. Diffusion of molecules and ions across lipid bilayer membrane.

Although nature has designed unique ways for the transport of ions across the cell membrane, mutations in genes can result in malfunction resulting in many diseases

like cystic fibrosis, myotonia, epilepsy etc. Design of synthetic ion transporters is in such a way that they compensate the malfunction of nature designed transport mechanism. Therefore, low molecular weight anion transporters mimicking the natural ion transport mechanism were developed and became an important topic in supramolecular chemistry.[2]

Mechanism of ion transport can be categorized into passive and active transport. Passive transport involves the movement of ions across the concentration gradient and happens through either symport, antiport or uniport. Active transport involves the transport of ions against the concentration gradient by utilizing energy. Co-transport is a transport mechanism in which among a gradient of solute, one is transported against its concentration gradient at the cost of another solute.

1.2. Natural anion transporters

In natural systems, usually, anion transport is mediated by natural ion channels present. Nevertheless, there are few known examples of natural anion transporters like prodigiosin (Figure 2). The proper functioning of natural ion channels or transporters is essential for the healthy survival of the cell.

Tambjamine   Prodigiosin
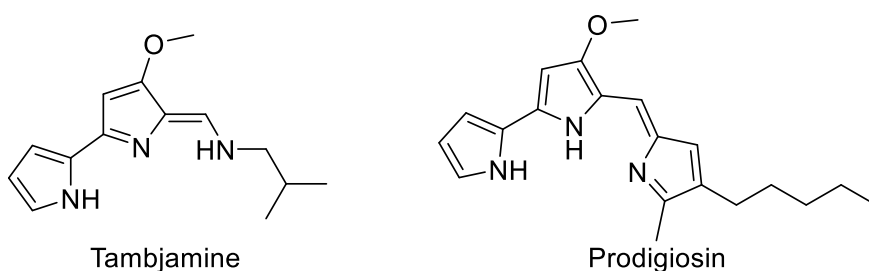
Figure 2. Natural small-molecule anion transporters.

1.3. Synthetic anion transporters

Synthetic anion transporters[3,4] are developed by designing molecules that bind to anions by hydrogen bond interactions, anion-π interactions etc. The efficiency of these molecules to bind to anions and their transport across lipid bilayer depends on the reversibility of binding.
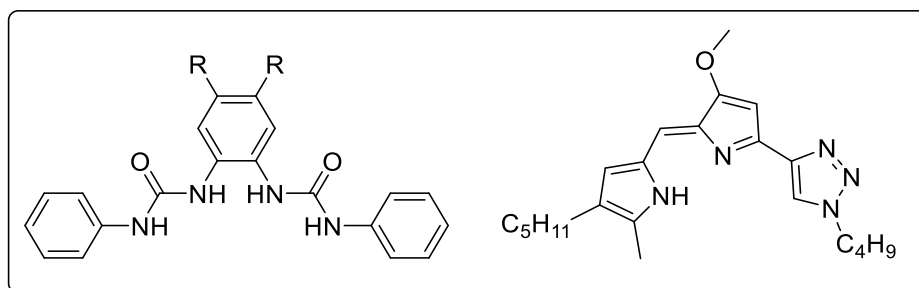
Figure 3. Synthetic small-molecule anion transporters.

There should be an optimum balance between lipophilic and hydrophobic nature of the molecule so that it can cope up with the membrane potential and transport anion across it. According to Lipinski rule, the logP value should be around 5 to make it an efficient anion transporter. Molecules are known to bind to anions like chloride, sulfate, bicarbonate, nitrate etc. Most important anions among them are nitrates and chlorides due to their effect on human health.

1.4. Nitrates in plant and human health

In nature, proteins and enzymes carry out nitrate uptake and metabolism. They have amino acid residues that contribute to ion pairing interactions and strong hydrogen bonding with nitrate and has maximum contact as well. The charge, hydrogen bond directionality, and shape of the cavity are very important for nitrate receptors and transporters.

Over the last two decades, numerous synthetic ion channels and carriers were developed for the selective transport of specific ions. However, a very few nitrate selective transporters were reported. Usually, nitrates are considered as benign to human health but these ions have some health benefits as well namely as (1) gastric protection, (2) oral/dental protection, (3) blood sugar regulation and (4) prevention from urinary tract infections.[5]

Nitrates in mammalian cells help in the regulation of various physiological functions via Nitrogen oxide cycle. Nitrates taken up by cells are reduced to nitrite by Xanthine oxidases and other enzymes in cells. These nitrites are further metabolized to nitric

oxide and other biologically active nitrogen oxides. This system acts as a backup for NO generation when NO synthases are malfunctioning that requires oxygen. This suggests therapeutic implications of nitrate to nitric oxide pathway in the given medical conditions like stroke, systemic, myocardial infarction and pulmonary hypertension, and gastric ulceration.[6,7,8]

Nitrates are essential for plants as well.[9] Various natural nitrate transporters (NRT) in plant cell mediate the nitrate transport in plant cells. In case of mutation and malfunction of the natural NRTs, synthetic small molecule nitrate transporters can mimic the natural NRT, hence resolving the issue to nitrate transport. Nitrate selective transporters are reported rarely owing to the complex binding of nitrate with the transporter.[5]

1.5. Light responsive anion transporter

In order to achieve spatial and temporal control over the anion transport, the compound should be responsive to certain stimuli. The protransporters reported here, can be specifically activated at the target of interest by utilizing light as a trigger. Light responsive anion transporters is also a very promising and emerging area in supramolecular chemistry. The active transporter is covalently attached to *o*-nitrobenzyl (ONB)[10] at one of the anion binding sites making it inactive for the transport. Light of wavelength 365 nm is used to phototrigger the release of the transporter release.
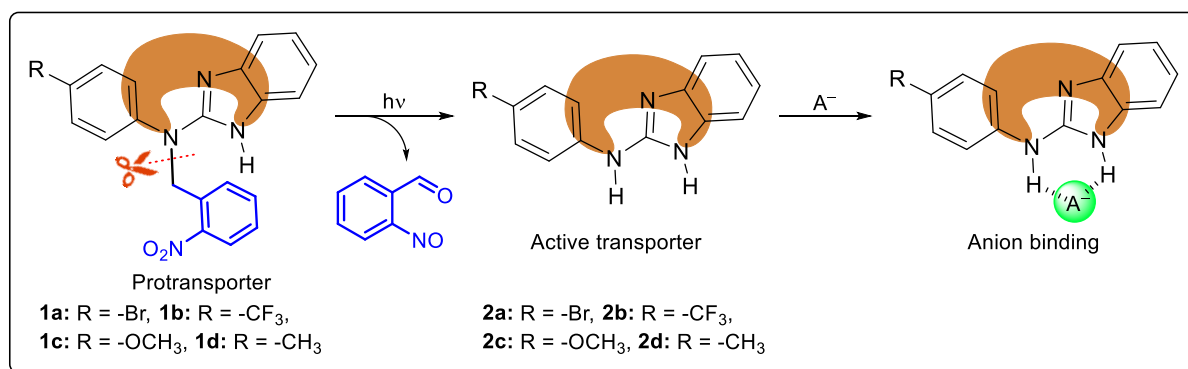

1a: R = -Br, 1b: R = -CF$_3$,
1c: R = -OCH$_3$, 1d: R = -CH$_3$

2a: R = -Br, 2b: R = -CF$_3$,
2c: R = -OCH$_3$, 2d: R = -CH$_3$

Figure 4. Schematic representation of photorelease of active transporter **2b** from **1b**.

2. Methods

2.1 Experimental Section

General Methods

Reagents and compounds used for the synthesis were purchased from Sigma-Aldrich, Avra chemicals, Spectrochem, Alfa Aesar and used without further purification. For dry reaction, CH_2Cl_2 and DMF were purchased from commercial suppliers and used without further purification.Egg yolk phosphatidylcholine, (EYPC) was purchased from Avanti Polar Lipids as a solution of 25 mg/mL in $CHCl_3$.

Physical Measurements

All ^1H NMR (400 MHz) and ^{13}C (100 MHz) spectra were recorded on Bruker 400 MHz and JEOL 400 MHz spectrometers. The chemical shifts ($δ$) in parts per million were referenced to the residual proton signal of deuterated solvents (^1H NMR $CDCl_3$: $δ$ 7.26 ppm; ^1H NMR DMSO-d_6: $δ$ 2.50 ppm; ^{13}C NMR DMSO-d_6: $δ$ 39.52 ppm). The multiplicities of the peaks are s (singlet), d (doublet), q (quartet), t (triplet), dd (doublet of doublet), m (multiplet). Column chromatography was performed using ethyl acetate in hexane as solvent on silica (100-200 mesh) and also methanol in chloroform as solvent on silica (100-200 mesh).

Ion transport activity using Lucigenin assay

Preparation of salt and stock solution for Lucigenin assay[11]

Salt solution was prepared by dissolving $NaNO_3$ (200 mM) in autoclaved water. Lucigenin dye was later added into this salt solution to make 1 mM solution of lucigenin. All the compounds were dissolved in HPLC grade CH_3CN solvent to make stock solutions.

Preparation of EYPC-LUVs ⊃ Lucigenin for ion transport activity:

1 mL off egg yolk phosphatidylcholine (EYPC, 25 mg/mL in CHCl₃) was taken in a round bottom flask. It was dried by purging nitrogen along with continuous rotation to form thin film of EYPC. Then round bottom flask was kept in high vacuum for 6 h to remove trace amount of CHCl₃. Later 1 mL solution(1 mM lucigenin, 200 mM NaNO₃) was added into the thin film to hydrate and was vortexed occasionally (4-5 times) for 1 h. Then it was subjected to freeze-thaw cycle (> 15 times). Extrusions were done using mini extruder with polycarbonate membrane (pore diameter of 200nm). All extra vesicular dyes were removed by gel filtration with Sephadex G-50 using same buffer without Lucigenin dye. The vesicle obtained was diluted to 6 ml using the same buffer to get EYPC-LUVs ⊃ Lucigenin ~ 5.0 mM EYPC; inside: 1 mM Lucigenin, 200 mM NaNO₃.Outside: 200 mM NaNO₃

Comparative Ion transport activity using Lucigenin assay:

In a clean and dry fluorescence cuvette, 1950 μL 100 mM NaNO₃ solution was taken and into it 25 μL of EYPC-LUVs ⊃HPTS was added and this cuvette was placed on fluorescence instrument equipped with magnetic stirrer (t = 0 s). Fluorescence emission intensity of Lucigenin dye, F_t was monitored at λ_{em} = 535 nm (λ_{ex} = 455 nm). Chloride ion concentration gradient was created between intra and extra vesicular system by adding 33 μL of 0.5 NaCl to the same cuvette at t = 50 s. Compounds were added at different concentration at t = 100 s each time and finally at t =300 s, 25 μL of 10% Triton-X-100 was added to lyse all the vesicles which resulted in the destruction of chloride ion concentration gradient and saturation of fluorescence intensity.

Fluorescence time courses (F_t) were normalized to fractional emission intensity I_F using Equation given below:

$$\% \text{ FI Intensity } (I_F) = [(F_t - F_0) / (F_\infty - F_0)] * (-100) \qquad \text{Equation S1}$$

where, F_0 = Fluorescence intensity just before the compound addition (at 0 s). F_∞ = Fluorescence intensity at saturation after complete leakage. F_t = Fluorescence intensity at time t.

Figure 5. Schematic representation of the lucigenin assay (**A**). Internal and external compositions used in the assay (**B**). Schematic representation of determination of ion transport activity using lucigenin assay (**C**).

Ion transport activity by symport assay:

In a clean and dry fluorescence cuvette, 1950 µL of salt solution (100 mM NaNO$_3$) was taken and into it 25 µL of EYPC-LUVs ⊃ HPTS was added and this cuvette was placed on fluorescence instrument equipped with magnetic stirrer (t = 0 s). Fluorescence emission intensity of Lucigenin dye, F$_t$ was monitored at λ$_{em}$ = 535 nm (λ$_{ex}$ = 455 nm). Then a chloride ion concentration gradient was created between intra and extra vesicular system by adding 33 µL of 2N MCl solution (where M$^+$ = Li$^+$, Na$^+$, K$^+$, Rb$^+$, Cs$^+$) to the same cuvette at t = 50 s. Compound was added at t = 100 s and finally at t = 300 s, 25 µL of 10% Triton-X-100 was added to lyse all the vesicles which resulted in the destruction of chloride ion concentration gradient and saturation of fluorescence intensity.

Fluorescence time courses (F$_t$) were normalized to fractional emission intensity I$_F$ using Equation given below:

$$\% \; Fl \; \text{Intensity} \; (I_F) = [(F_t - F_0) / (F_\infty - F_0)] * (-100) \qquad \text{Equation S1}$$

Where F_0 = Fluorescence intensity just before the compound addition (at 0 s). F_∞ = Fluorescence intensity at saturation after complete leakage. F_t = Fluorescence intensity at time *t*.
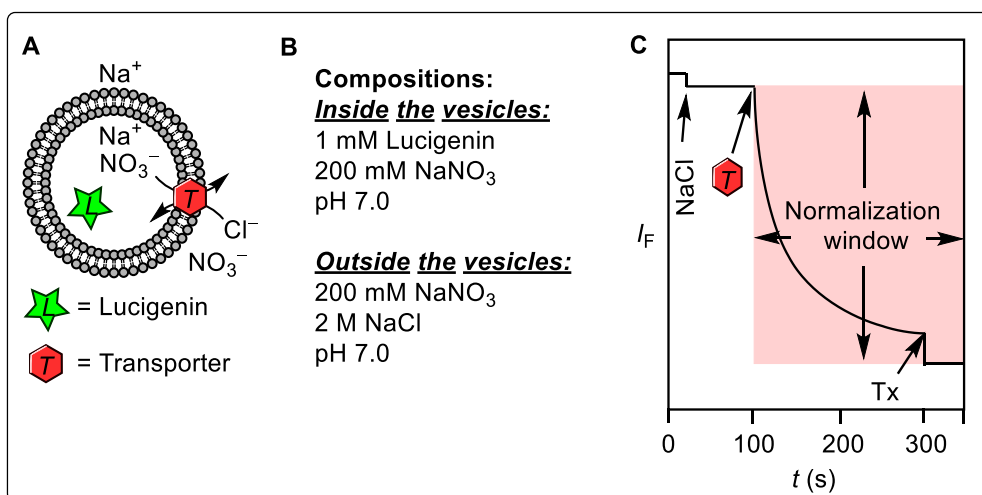
Figure 6. Schematic representation of cation dependence in the lucigenin assay.

Ion transport activity by antiport assay using valinomycin:

In a clean and dry fluorescence cuvette, 1950 μL 100 mM NaNO$_3$ solution was taken and into it 25 μL of EYPC-LUVs ⊃HPTS was added and this cuvette was placed on fluorescence instrument equipped with magnetic stirrer (t = 0 s). Fluorescence emission intensity of Lucigenin dye, F_t was monitored at λ$_{em}$ = 535 nm (λ$_{ex}$ = 455 nm). Then a chloride ion concentration gradient was created between intra and extra vesicular system by adding 33 μL of 2N KCl to the same cuvette at t = 20 s. Later, 0.5 μM valinomycin was added at t = 50 s. 18 μL of 500 μM compound solution was added at t = 100 s and finally at t = 300 s, 25 μL of 10% Triton-X-100 was added to lyse all the vesicles which resulted in the destruction of chloride ion concentration gradient and saturation of fluorescence intensity.

Fluorescence time courses (F_t) were normalized to fractional emission intensity I_F using Equation given below:

$$\% \, Fl \text{ Intensity } (I_F) = [(F_t - F_0) / (F_\infty - F_0)] * (-100) \qquad \text{Equation S1}$$

Where F_0 = Fluorescence intensity just before the compound addition (at 0 s). F_∞ = Fluorescence intensity at saturation after complete leakage. F_t = Fluorescence intensity at time *t*.
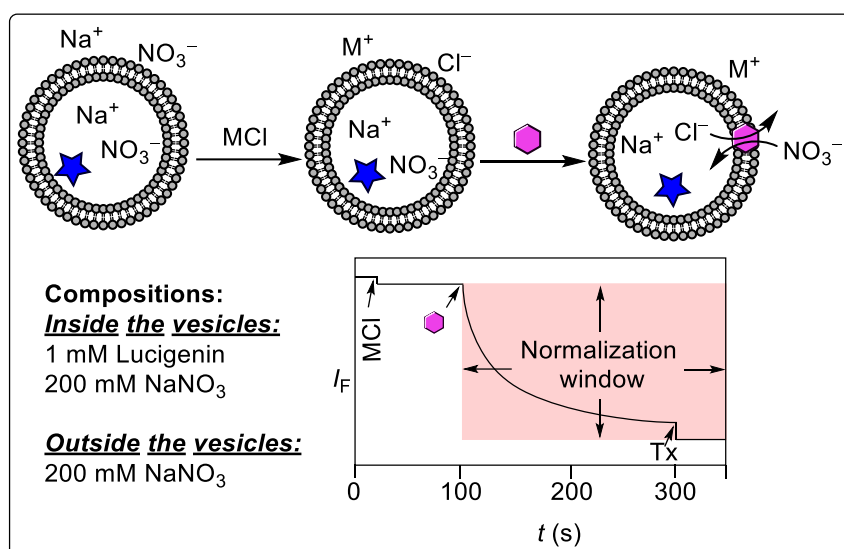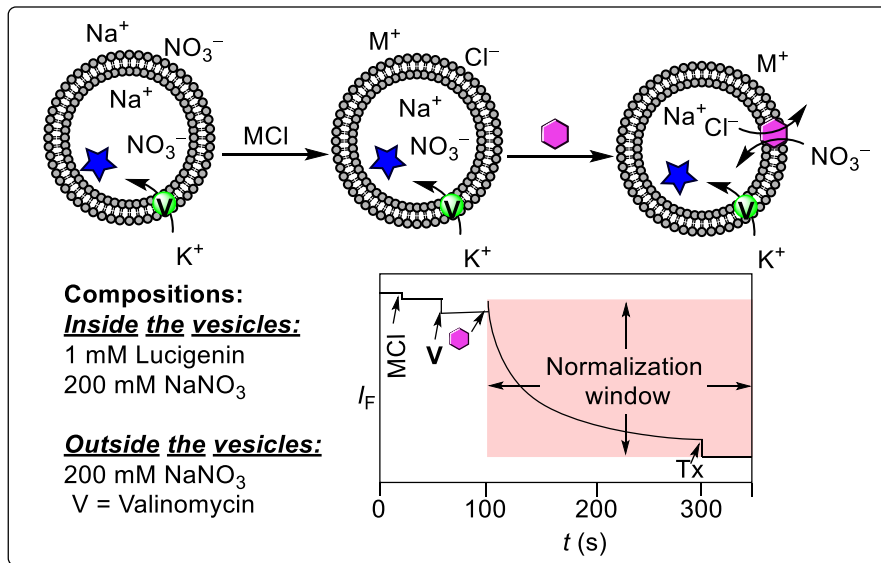
Figure 7. Schematic representation of valinomycin coupled nitrate efflux assay.

A. Ion transport activity studies across EYPC-LUVs⊃HPTS:

Preparation of HEPES buffer and stock solutions: The HEPES buffer of pH = 7.0 was prepared by dissolving an appropriate amount of solid HEPES (10 mM) and NaCl (100 mM) in autoclaved water. The pH was adjusted to 7.0 by addition aliquots from 0.5 M NaOH solution. The stock solution of all carriers was prepared using HPLC grade DMSO.

Preparation of EYPC-LUVs⊃HPTS in NaNO₃: In 10 mL clean and dry round bottom flask thin transparent film of egg yolk phosphatidylcholine (EYPC) was formed using a 1 mL EYPC lipid (25 mg/mL in $CHCl_3$) by providing continuous rotation and purging nitrogen gas. The transparent thin film was completely dried under high vacuum for 4-5 h. After that transparent thin film was hydrated with 1 mL HEPES buffer (1 mM HPTS, 10 mM HEPES, 100 mM $NaNO_3$, pH = 7.0) and resulting suspension was vortexed at 10 min intervals during 1 h. This hydrated S15 suspension was subjected to 15 cycles of freeze-thaw (N₂ gas, 55 °C) followed by extrusion through 100 nm (pore size) polycarbonate membrane for 21 times, to obtain the vesicles of an average 100 nm diameter. The unentrapped HPTS dyes were removed by size exclusion chromatography using Sephadex G-50 (Sigma-Aldrich) with eluting of HEPES buffer (10 mM HEPES, 100 mM $NaNO_3$, pH = 7.0). Finally, collected vesicles were diluted to 6 mL to get EYPC-LUVs⊃HPTS. *Final conditions: ~ 5 mM EYPC, Inside: 1 mM HPTS,*

10 mM HEPES, 100 mM NaNO$_3$, pH = 7.0, Outside: 10 mM HEPES, 100 mM NaNO$_3$, pH = 7.0.

Ion transport activity by HPTS assay:

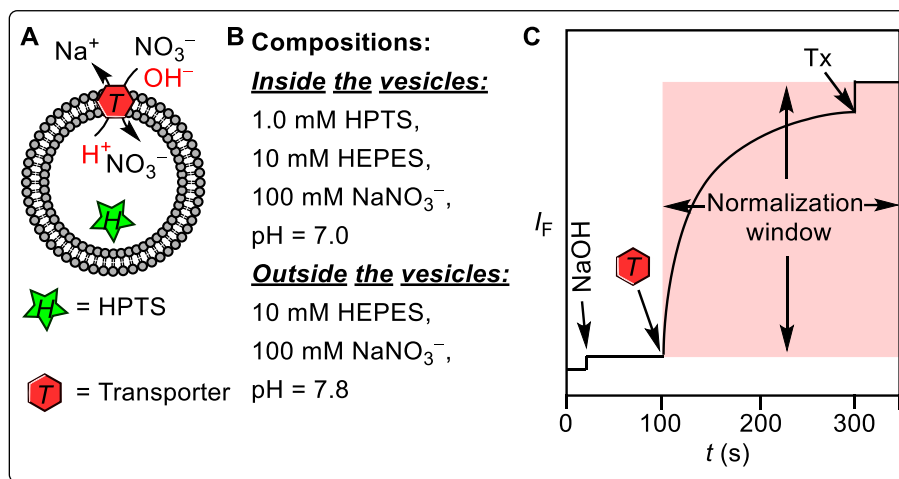*Figure 8*. Representations of fluorescence-based ion transport activity assay using EYPC-LUVs⊃HPTS (**A**), Internal and external compositions used in the assay (**B**) and illustration of ion transport kinetics showing normalization window (**C**).

 In clean and dry fluorescence cuvette, 1975 µL of HEPES buffer (10 mM HEPES, 100 mM NaNO$_3$, pH =7.0) and 25 µL of EYPC-LUVs⊃HPTS vesicle was added. The cuvette was placed in slowly stirring condition using magnetic stirrer equipped in fluorescence instrument (*t* =0 s). The time-dependent HPTS emission intensity monitored at λ_{em} = 510 nm (λ_{ex} = 450 nm) by creating pH gradient between intra- and extra- vesicular system by addition of 0.5 M NaOH (20 µL) at *t* = 20 s. Then different concentrations of transporter molecules in DMSO were added at *t* =100 s. Finally, the vesicles were lysed by addition of 10% Triton X-100 (25 µL) at *t* = 300 s to disturbed pH gradient. The time axis was normalized according to Equation S2:

$$t = t - 100 \qquad \qquad \text{Equation S2}$$

The time-dependent data was normalized to percent change in fluorescence intensity using Equation S3:

$$I_F = [(I_t - I_0) / (I_\infty - I_0)] \times 100 \qquad \qquad \text{Equation S3}$$

Where, I_0 is the initial intensity, I_t is the intensity at time t, and I_∞ is the final intensity after addition of Triton X-100.

Dose-response activity: The fluorescence kinetics of each transporter at different concentration was studied as a course of time. The concentration profile data were evaluated at $t = 290$ s to get effective concentration, EC_{50} (i.e. the concentration of transporter needed to achieve 50% chloride efflux) using Hill equation (Equation S4):

$$Y = Y_\infty + (Y_0 - Y_\infty) / [1 + (c/EC_{50})^n] \qquad \text{Equation S4}$$

where, Y_0 = fluorescence intensity just before the transporter addition (at $t = 0$ s), Y_∞ = fluorescence intensity with excess transporter concentration, c = concentration of transporter compound, and n = Hill coefficient (i.e. indicative for the number of monomers needed to form an active supramolecule).

Phototriggered activation and ion transport assay in LUVs: In clean and dry fluorescence cuvette, 1975 μL HEPES buffer (10 mM HEPES, 100 mM NaNO$_3$, pH = 7.0) and 25 μL EYPC-LUVs⊃HPTS vesicles were placed. To this suspension, either carrier **2b** (20 μL) or procarrier **1b** (20 μL) was added to get a final concentration of 200 nM. For procarrier **1b**, the suspension was irradiated with 365 nm wavelength UV (using three 3W LEDs each placed at a distance of 2 cm) for time, $t_R = 0, 1, 5, 10, 20$, and 30 min. Each irradiated sample was then placed in the fluorescence instrument equipped with a magnetic stirrer. The fluorescence intensity of HPTS at $\lambda_{em} = 510$ nm ($\lambda_{ex} = 450$ nm) of each sample was monitored as a course of time t. At $t = 100$ s, a pH gradient was created by the addition of 20 μL NaOH (0.5 M). Finally, at $t = 300$ s vesicles were lysed by the addition of 10% Triton X-100 (25 μL) to get the complete destruction of the applied pH gradient. Each, time-dependent fluorescence data was normalized using Equation S3. A sample containing 1975 μL HEPES buffer (10 mM HEPES, 100 mM NaNO$_3$, pH = 7.0), 25 μL EYPC-LUVs⊃HPTS and 20 μL DMSO was also subjected to 5 min irradiation with same UV LEDs. The ion transport activity of this sample was measured by adding 20 μL NaOH (0.5 M) at $t = 100$ s of the kinetics experiment, and this data was used as a control data. The time axis was normalized according to Equation S2. The time-dependent data were normalized to percent change in fluorescence intensity using Equation S3.

3. Results and Discussion

Synthesis of active transporters 2a-2d:

According to the proposed design, we synthesized four derivatives of the benzimidazole core based active transporters which bind anions via non-covalent N-H···A⁻ bonds and transports anions across lipid bilayer membrane of vesicles. Compounds **2a-2d** were synthesized by reacting 2-chloro-1*H*-1,3-benzodiazole **7** with the corresponding aniline in the presence of catalytic amount of HCl in ethanol to give good yields.
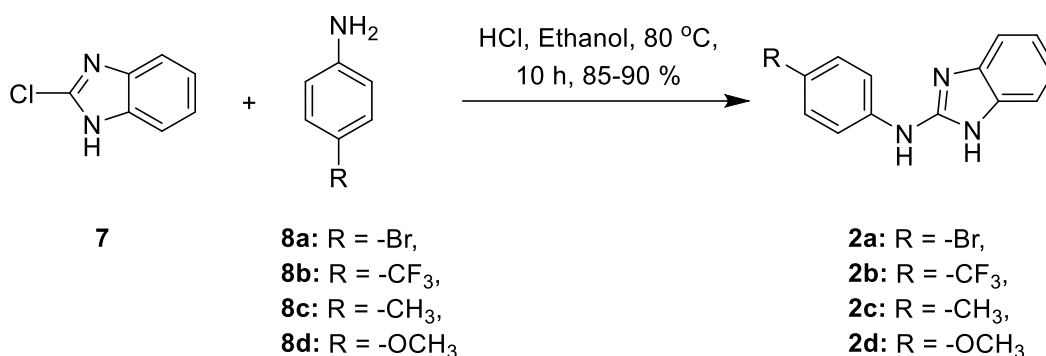
Scheme 1. Scheme of synthesis of benzimidazole core based transporters **2a-2d**.

Compound	R group	logP	pK$_{a1}$	pK$_{a2}$
2a	Br	4.5	17.96	11.85
2b	CF$_3$	4.59	17.96	11.98
2c	CH$_3$	4.22	18.44	11.85
2d	OCH$_3$	3.57	19.01	11.85

Table 1. Estimated logP and pK$_a$ values of **2a-2d**.

According to the calculations done by MarvinView 5.8 software,[12] we got above logP values which suggest **2b** and **2a** to be better transporters as compared to the other two. This is also supported by the pKa values as pKa$_1$ values for these are low as

compared to the remaining **2c** and **2d**. To get the best transporter of the given compounds the activity comparison was done in lucigenin and HPTS assay.

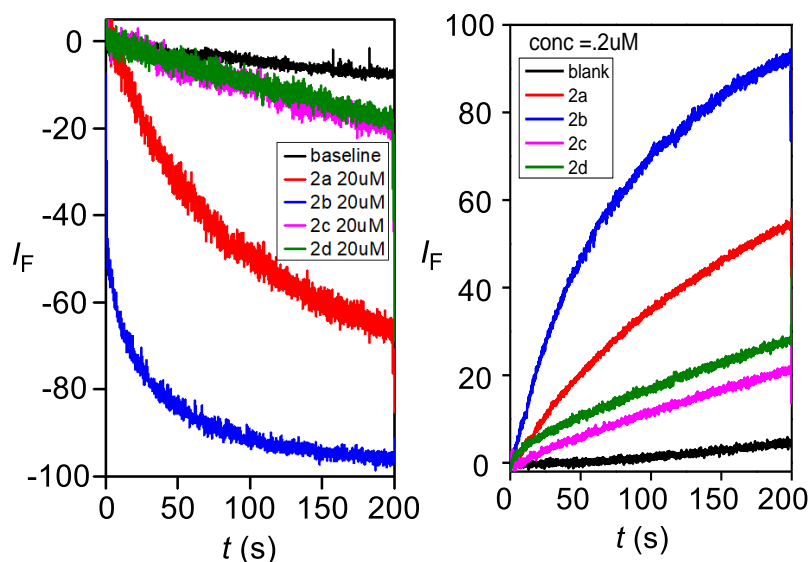**Ion transport activity comparison by Lucigenin and HPTS assay for 2a-2d:**

Figure 9. Comparison of active transporter **2a-2d** in lucigenin assay at 20 µM and HPTS assay with NaNO$_3$ salt at 0.2 µM.

In each of the above two comparisons **2b** came out to be most active so the anion selectivity was compared for different anions for compound **2b**.

Ion selectivity by HPTS assay for 2b:

For the comparison of anion selectivity of **2b**, extravesicular and intravesicular salts were changed so that there is the same anion outside and inside vesicles. The EYPC-LUVs vesicles were prepared with internal HPTS dye and 5 mM Na$^+$A$^-$ salt (A$^-$ = Cl$^-$, Br$^-$, I$^-$, ClO$_4^-$, NO$_3^-$), and then suspended in Na$^+$A$^-$ solution. The pH gradient was brought by the addition of NaOH followed by the addition of **2b**. Fluorescence intensity was recorded by fluorescence kinetics experiment. At 0.2 µM concentration, **2b** was found to be most selective for NO$_3^-$ as shown in the following figure. Nitrate and iodide have similar rates of transport for initial few seconds, then the iodide rate seems to decrease. This decrease in fluorescence intensity is due to partial quenching of HPTS

fluorescence by the iodide anion.[13] For cation selectivity, extravesicular salt changed MNO_3 (M = Li⁺, K⁺, Cs⁺, Na⁺) keeping intravesicular salt to $NaNO_3$. No change for different cations was observed implying that **2b** is not selective for cations.
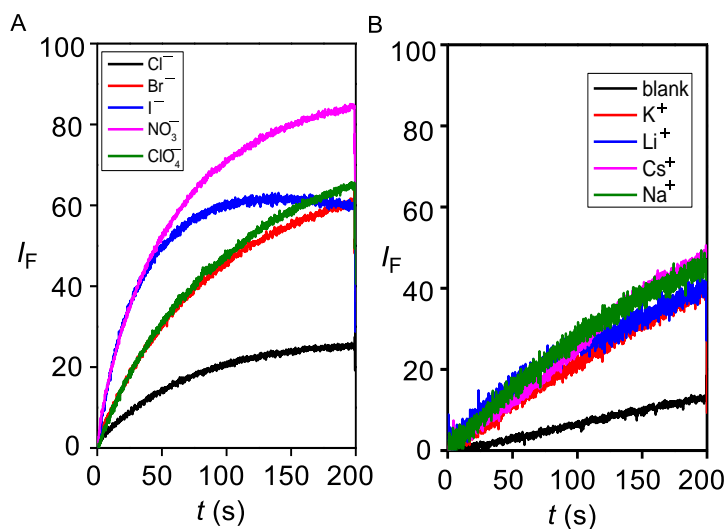

Figure 10. Anion selectivity of **2b** (0.3 µM) measured by varying the external anions of EYPC-LUVs⊃HPTS (**A**). Cation selectivity of **2b** (0.1 µM) measured by varying external cations (M⁺ = Li⁺, Na⁺, K⁺, Cs⁺) across EYPC-LUVs⊃HPTS (**B**).

Anion Binding Studies - ¹H NMR Titration:

To check the binding affinity of **2a-2d** with various anions, ¹H NMR titration experiment was performed. Since the compound was better transporter for NO_3, so **2a-2d** were titrated with $TBANO_3$. With the downfield shift of two NH protons present in active compounds, it is evident that anions bind to the NO_3 ion by NH---NO_3 hydrogen bond interactions. Similarly, titration with other anions indicated that all the anions bind via hydrogen bonding interactions. [**A**⁻] / ([**2a-2d**] + [A⁻]) was plotted against $\Delta\delta*$[**2a-2d**] / ([**2a-2d**] + [A⁻]) to obtain jobs plot. Change in chemical shift of NH_b was used to obtain

jobs plot (Figure 11) and Bindfitv0.5 online page[14] was used to calculate binding constant.

Compounds	Binding constants (M^{-1})			
Ions	Cl^-	NO_3^-	Br^-	I^-
2a		0.18		
2b	1.08	0.12	0.2	0.06
2c		*ND*		
2d		0.07		

ND = Could not be determined.

Table 2. Binding constant values calculated by ^1H NMR titration experiment.

Although the binding constant of **2a** is better than **2b** for nitrate anion, better transport efficiency of **2b** can be attributed to better logP value of the later.
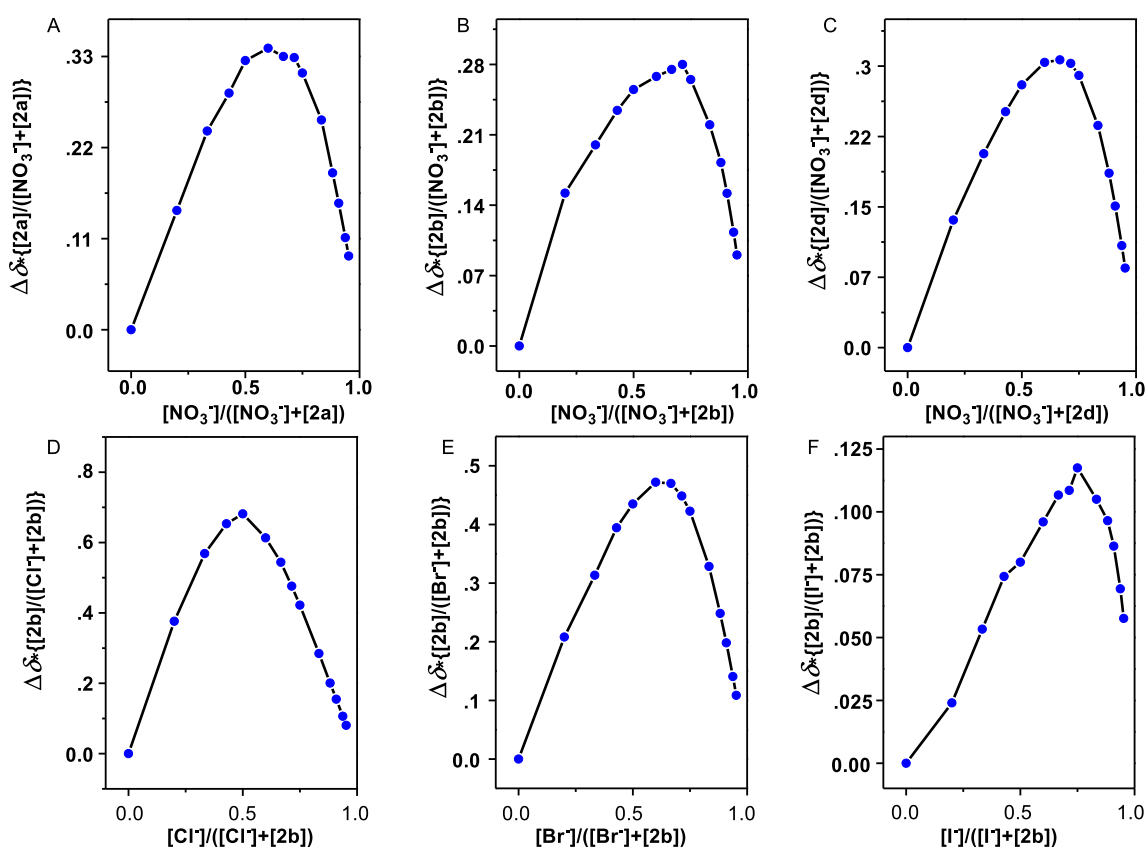
Figure 11. Job plot analysis for the N-H$_a$ proton shift of **2a, 2b** and **2c** upon titration with TBANO$_3$ (**A**), (**B**) and (**C**) upon titration with TBACl. Job plot analyses for the N-H$_a$ proton shift of **2b** upon titration with TBACl (**D**), TBABr (**E**), and TBAI (**F**).

From the Job plot analysis of **2b** for nitrate ion, $\Delta\delta$ came out to be maximum at 0.75, confirming that three molecules of **2b** bind with one molecule of NO_3 anion (Figure 11(B)) while $\Delta\delta$ was found to be maximum at ~ 0.66 indicating 2:1 binding of **2b** with chloride (Figure 11(D)). It suggested that two molecules of **2b** come together to bind one chloride ion. The binding constant values of various compounds with different anions are tabulated in Table 2 given above. (Binding constant for **2c** with nitrate ion could not be calculated, as the change in chemical shift of NH peak in NMR titration was insufficient).

The concentration profile was done for the compound **2b** to reveal the EC_{50} value (half maximal effective concentration) of **193.6 nM** (Figure 12) for the nitrate transport and **656 nM** (Figure 13) for the chloride transport. Hill coefficient **n = 2.97** for nitrate and **n = 1.88** for chloride, suggests that 3 molecules of **2b** are involved in the host guest complex formation in nitrate transport across the lipid bilayer membrane. Similarly, 2 molecules of **2b** are involved in chloride transport. The above-mentioned results obtained from the ^1H NMR titration (Table 2) of **2b** supports the Hill coefficient value obtained from the concentration profile of **2b**.
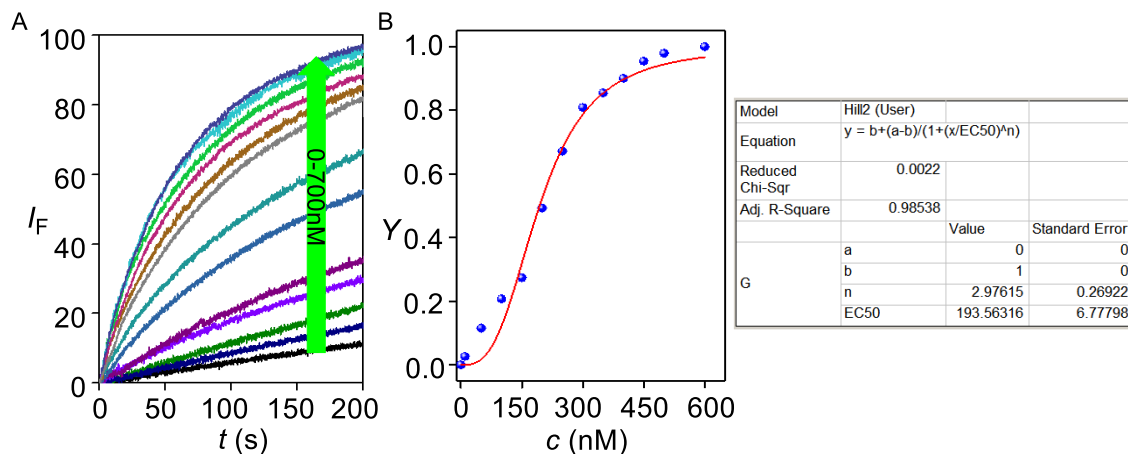

Figure 12. Concentration-dependent activity of **2b** across EYPC-LUVs⊃HPTS with isoosmolar (100 mM) $NaNO_3$ salt(**A**). Hill plot analysis of **2b** at t = 290 s (**B**).
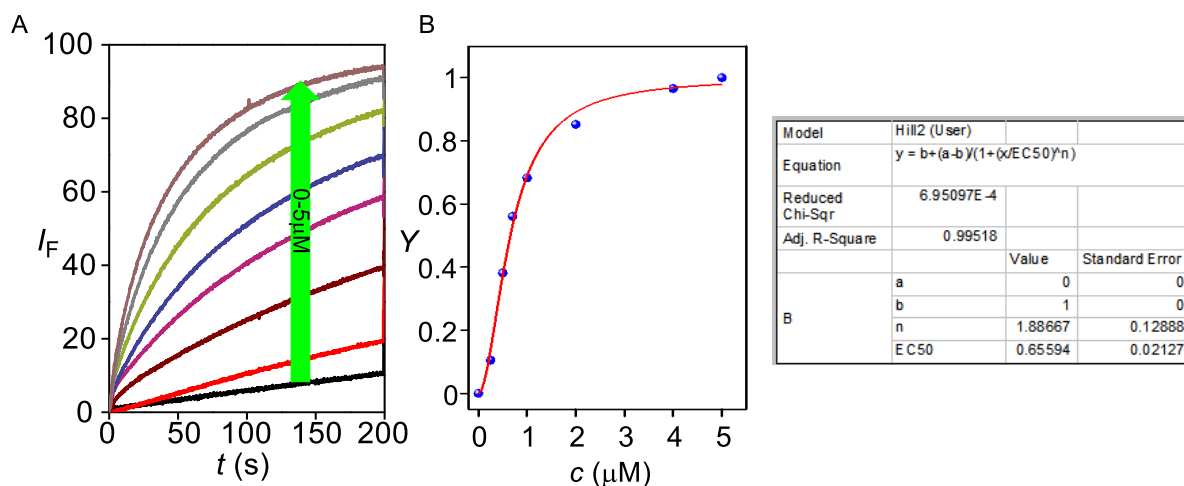
Figure 13. Concentration-dependent activity of **2b** across EYPC-LUVs⊃HPTS with isoosmolar (100 mM) NaCl salt (**A**). Hill plot analysis of **2b** at t = 290 s (**B**).

Determination of transport mechanism using Lucigenin assay:

In the lucigenin assay, transport of ions can take place either via Na^+/Cl^- symport mechanism or via Cl^-/NO_3^- antiport mechanism. In order to investigate the mechanism of transport, firstly the lucigenin assay was carried out by varying extravesicular salt of chloride (M^+Cl^-) (M^+ = Na^+, K^+, Li^+, Rb^+, Cs^+) of 2N concentration. Ion transport activity of **2b** was checked at **10 µM** concentration. No significant change in intensity was observed in different cation salts confirming that cations are not involved in ion transport. Next, to check if the transport mechanism is antiport, the lucigenin assay was done in the presence of valinomycin. Valinomycin is a selective K^+ ion transporter. So if the transport mechanism is antiport then in the presence of valinomycin **2b** will have enhanced transport rates. Here, 2N KCl was taken as the extravesicular medium in the lucigenin assay. Firstly, chloride influx was checked at **0.2 µM** valinomycin. For measuring the effect of valinomycin on chloride influx, the chloride influx of **2b** was measured with and without valinomycin (0.2 µM). As it is evident from Figure 14(A), no change in the rate of chloride influx was observed. This confirms that **2b** is not transporting anions via chloride/nitrate antiport mechanism but the proton coupled anion transport is happening i.e., co- transport of H^+ and NO_3^- is happening.
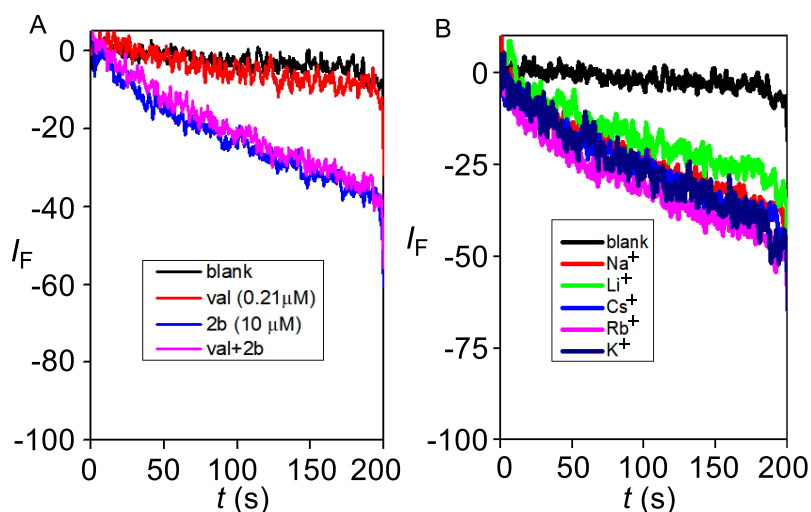
Figure 14. Lucigenin with and without valinomycin antiport assay (**A**). Lucigenin assay using different extravesicular cations.(**B**)

Synthesis of protransporter 1b:

After the comparison between the ion transport activities of **2a-2d**, it was confirmed that **2b** is the best ion transporter so the protransporter for **2b** was synthesized. In a 50 mL round bottomed flask, **2b** (1 eq) was dissolved in acetone and *o* –nitrobenzyl bromide (1.25 eq) was added to the solution. A catalytic amount of KOH was added to the reaction mixture and heated at 80 ºC for 10 hours. After reaction completion, the solvent was evaporated in *vacuo*. Then the reaction was extracted in EtOAc and washed thrice with water. The crude product obtained was purified by column chromatography (10% MeOH/CHCl₃) to obtain pure **1b** in good yields.
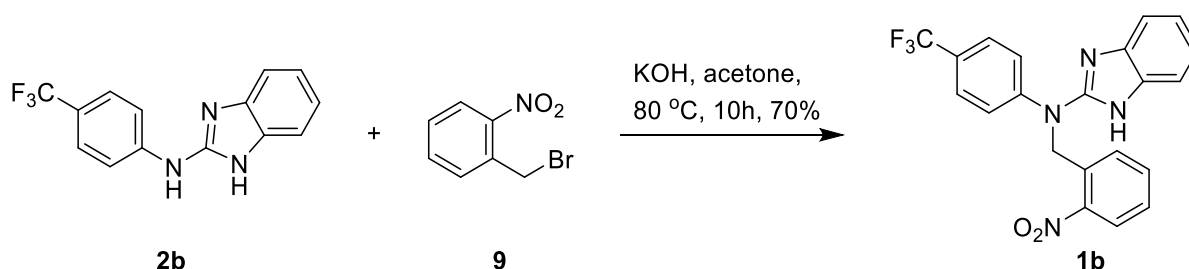
Scheme 2. Synthesis of protransporter **1a**.

Comparison between anion transport activity of active and pro transporter

In order to check if protecting one for the binding sites for anion has rendered the compound inactive for the transport, we compared the anion transport activity of both

23

compounds at 0.1 µM in HPTS assay. The experiment showed that in protransporter in unable to transport the anions across the lipid bilayer (Figure 15).

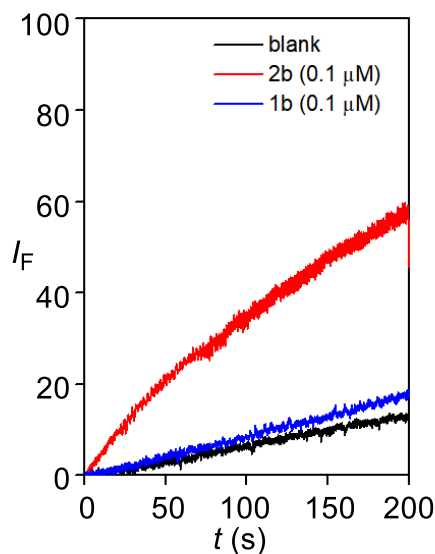*Figure 15.* Comparison between active **2b** (0.1 µM) and protransporter **1b** (0.1 µM) in the HPTS assay.

Phototriggered activation of protransporter 1b and ion transport assay in LUVs

The phototriggered activation of the protransporter **1b** (0.2 µM)was checked according to the procedure mentioned above in the methods section. This experiment showed successful cleavage of the ONB (*o*-nitrobenzyl)[15] group after irradiation with the light of wavelength 365 nm and regain of ion transport as **2b** was regenerated. Around 80 percent of the transport activity as compared to the active transporter **2b** was recovered after irradiation as plotted in Figure 16B.
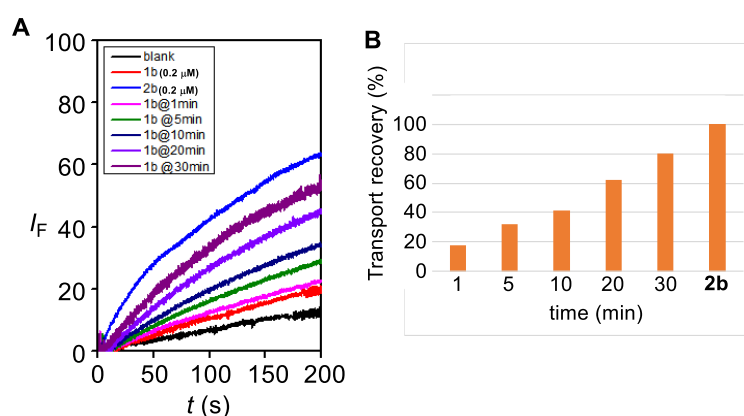
Figure 16. Normalized ion transport activity data upon photoirradiation (**A**). Bar diagram showing percent clevage with respect to time(**B**).

4. Conclusions

We successfully synthesized benzimidazole core based transporters **2a-2d**. The involvement of protons of **2b** was investigated by ^{1}H NMR titration indicating in both NH protons present in compound to be involved in binding. In activity comparison **2b** was found to be the most active transporter for nitrate anion with **EC_{50} = 193.56 nM**. The transport of the nitrate anion across the lipid bilayer happens in form of **3:1** complex formed by compound **2b** and 1 nitrate anion. Since **2b** was most active nitrate transporter so the protransporter **1b** was synthesized which was inactive for anion transport as hypothesized. The transport mechanism active in the **2b** is HNO_3 co-transport. Further, **1b** was subjected to photolysis studies by irradiation with 365 nm wavelength light. The ONB (*o*-nitrobenzyl) group of **1b** was cleaved and active compound **2b** was regenerated. The regenerated **2b** showed ion transport when transport studies were done. So in conclusion, we successfully synthesized selective nitrate transporter and corresponding protransporter 1b that are lesser known in literature, providing spatiotemporal control over the transport essential for a compounds biomedical application.

5. NMR titration figures
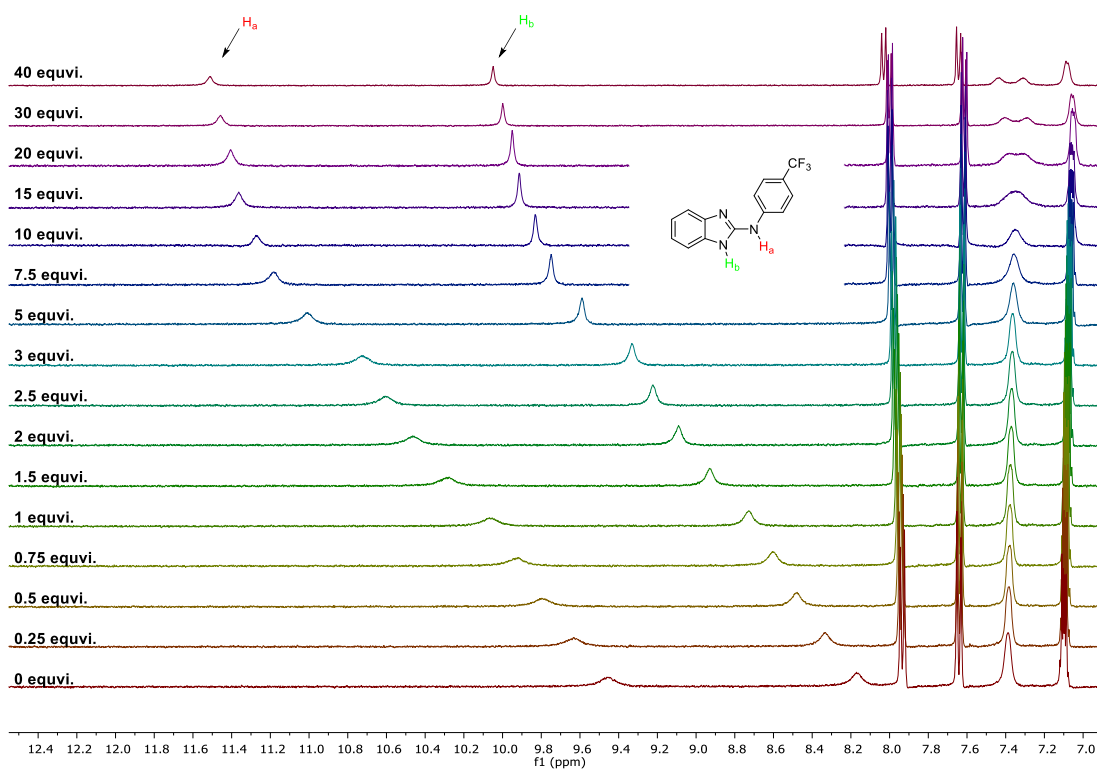
Figure 17. ^{1}H NMR titration spectra for **2b** (5 mM) with stepwise addition of TBANO$_3$ in CD$_3$CN. The equivalents of added TBANO$_3$ are shown on the stack spectra.

Figure 18. ^{1}H NMR titration spectra for **2a** (5 mM) with stepwise addition of TBANO$_3$ in CD$_3$CN. The equivalents of added TBANO$_3$ are shown on the stack spectra.
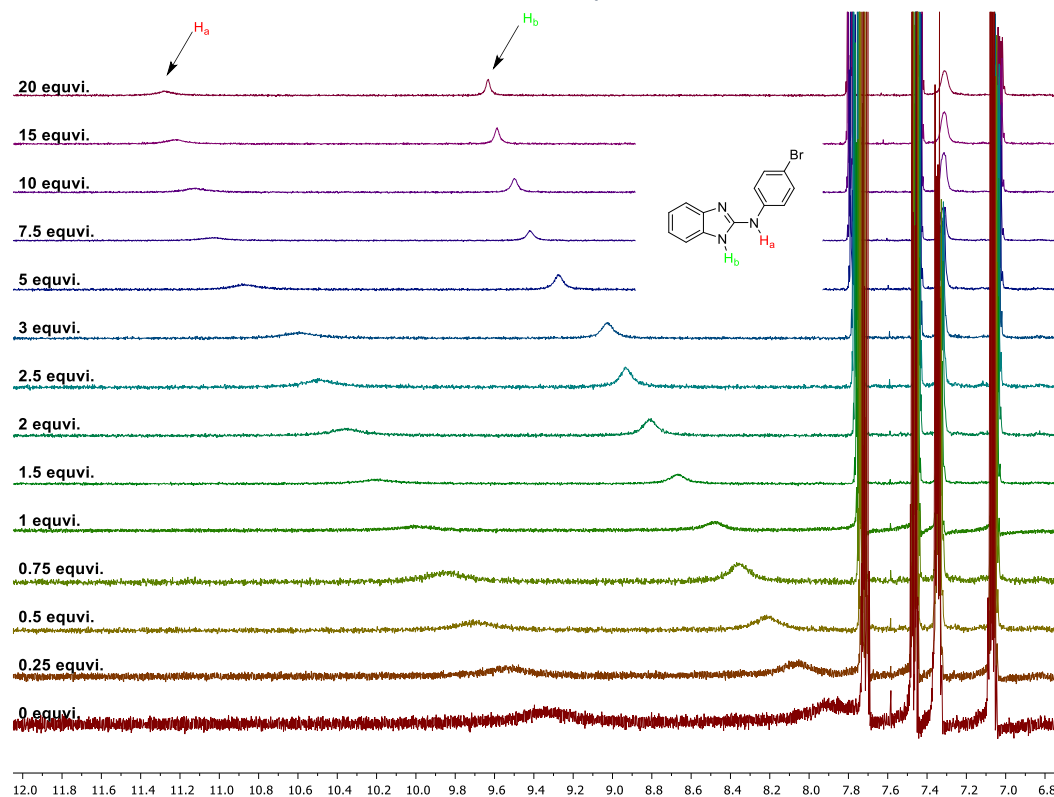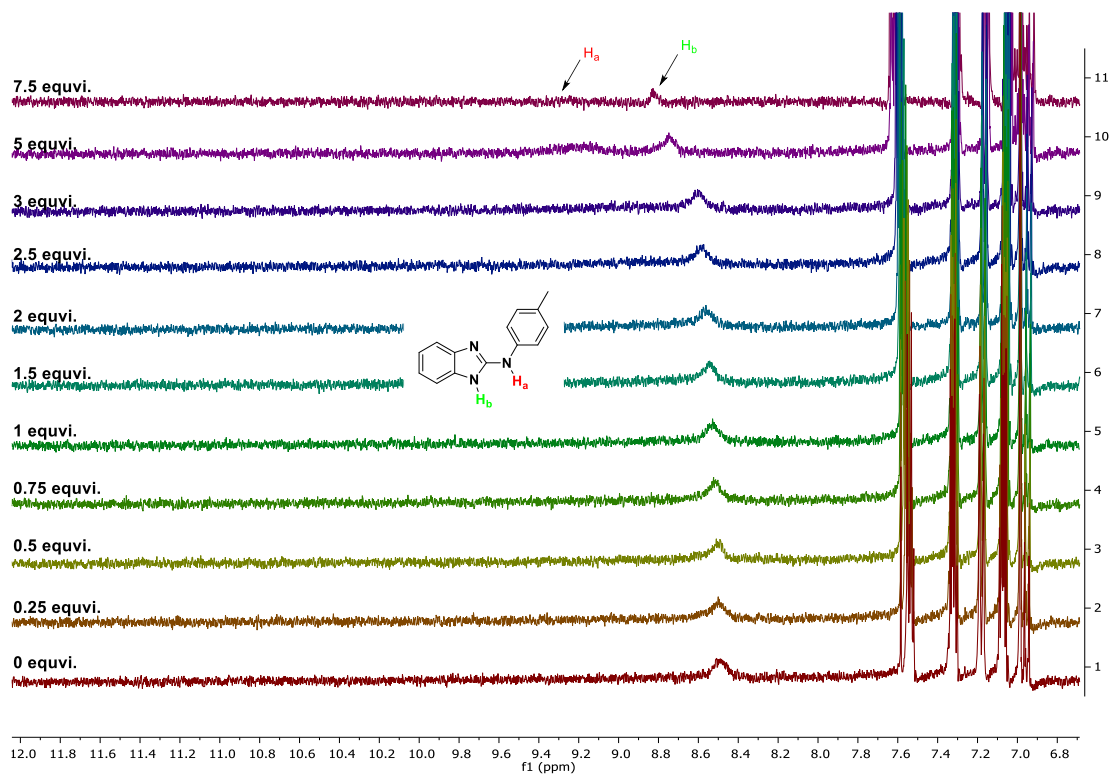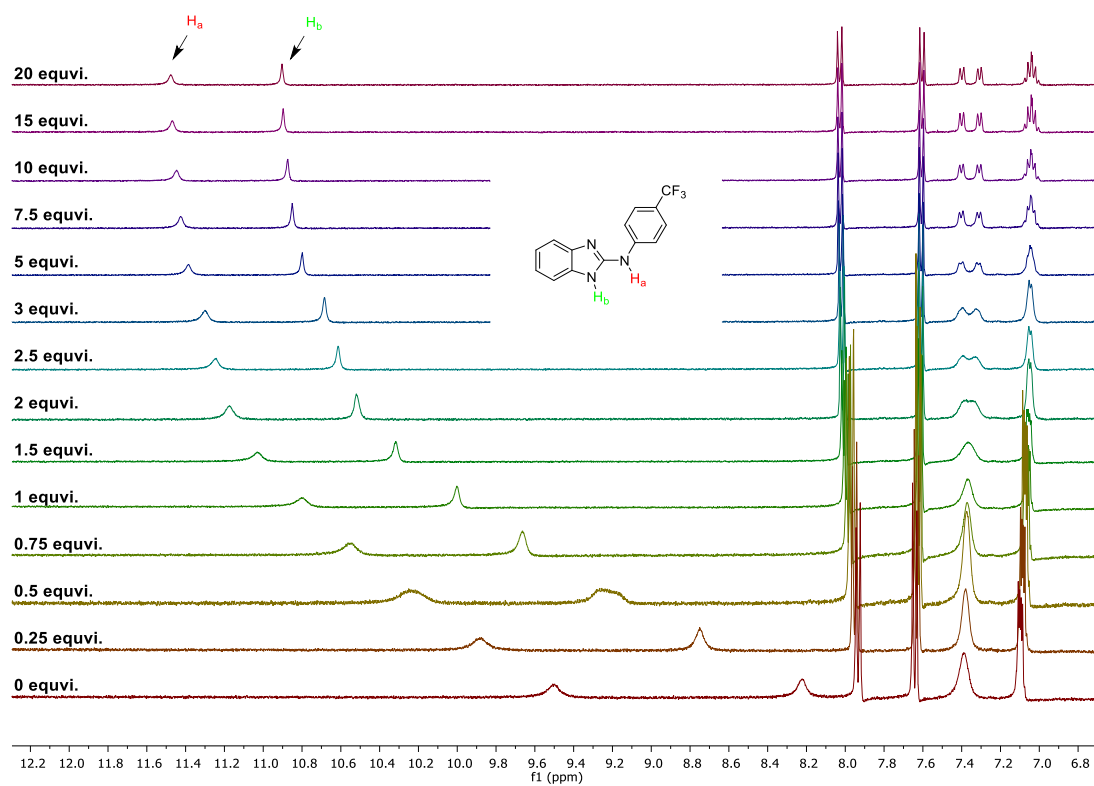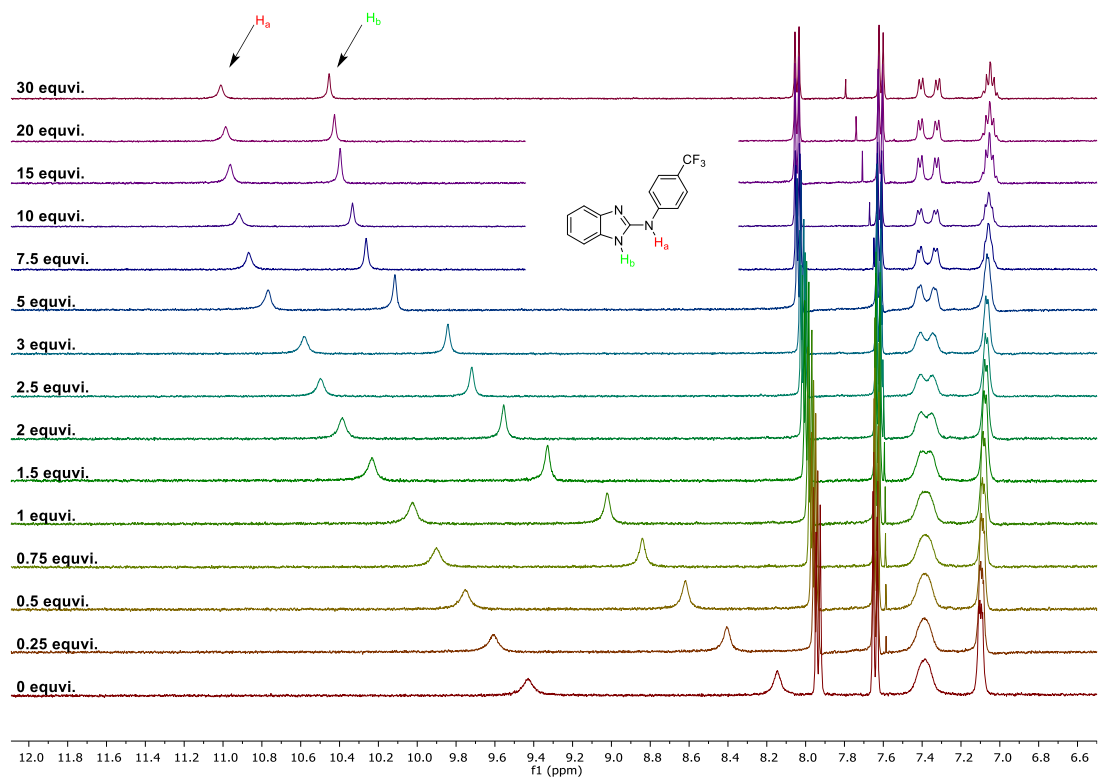
Figure 19. ^{1}H NMR titration spectra for **2c** (5 mM) with stepwise addition of TBANO$_3$ in CD$_3$CN. The equivalents of added TBANO$_3$ are shown on the stack spectra.

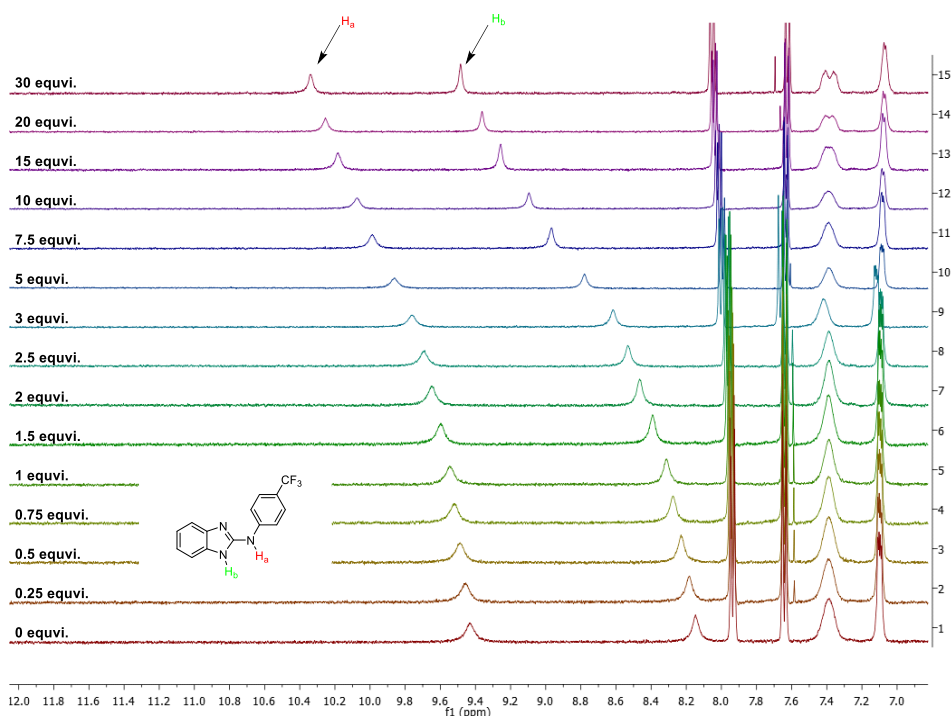*Figure 20.* ^{1}H NMR titration spectra for **2b** (5 mM) with stepwise addition of TBACl in CD$_3$CN. The equivalents of added TBACl are shown on the stack spectra.
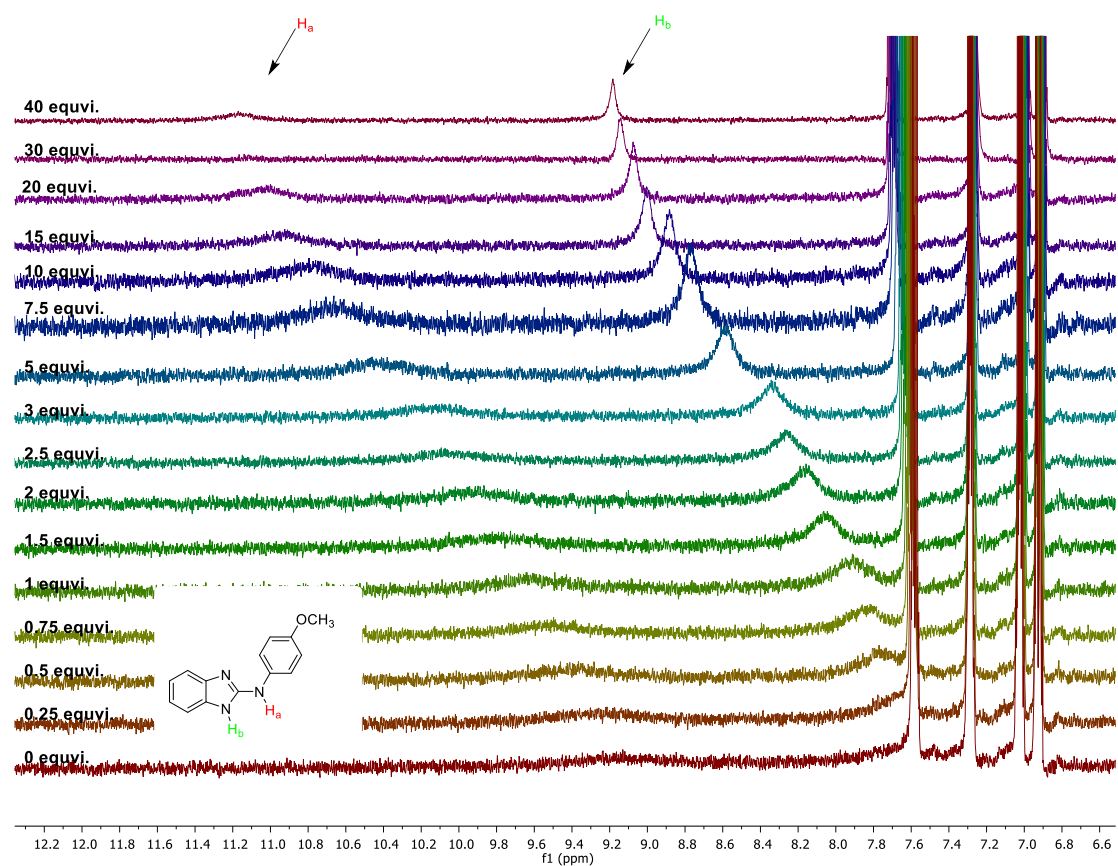
Figure 21 ^{1}H NMR titration spectra for **2d** (5 mM) with stepwise addition of TBANO$_3$ in CD$_3$CN. The equivalents of added TBANO$_3$ are shown on the stack spectra.

Figure 22. ^{1}H NMR titration spectra for **2b** (5 mM) with stepwise addition of TBABr in CD$_3$CN. The equivalents of added TBABr are shown on the stack spectra.

Figure 23. ^{1}H NMR titration spectra for **2b** (5 mM) with stepwise addition of TBAI in CD$_3$CN. The equivalents of added TBAI are shown on the stack spectra.

Synthesis of 1,3-dihydro-benzimidazole-2-one 6
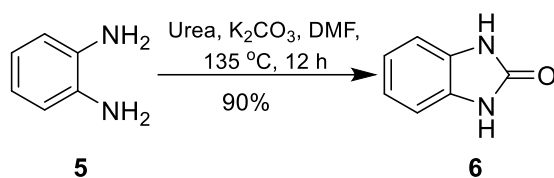
Compound **6** was prepared according to the reported procedure. Firstly, 1,2-diaminobenzene **5** (2 g, 18.49 mmol) was dissolved in DMF (20 mL). Urea (2.22 g, 36.99 mmol) was next added to the solution and stirred overnight at 135 °C. After the reaction completion, DMF was removed in *vacuo*, the separated solid was given was with water. Separated solid was dissolved in 10% NaOH solution. The aqueous alkaline solution was filtered and neutralized with 35% HCl. The separated solid was filtered, washed and dried to obtain pure 1,3-dihydro-benzimidazole-2-one **6**. Yield: 90%. NMR data is matching with reported data.[16]

## Synthesis of 2-chloro-1H-benzimidazole 7
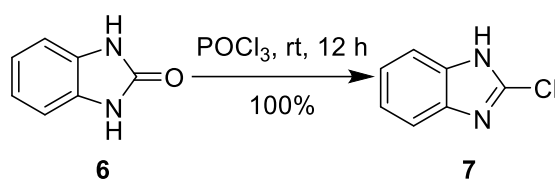
A mixture of **6** (2 g, 14.91 mmol) and 2.79 mL (29.82 mmol) POCl$_3$ was stirred at rt for 12 hours. After the reaction completion, the mixture was treated with xylene to remove excess POCl$_3$. The reaction mixture was cooled in ice and neutralized in 40% NaOH to pH = 10.0. The separated crude was recrystallized to get pure 2-chloro-1*H*-benzimidazole **7**. Yield: 100%. NMR data is matching with reported data.[16]

## Synthesis of active benzimidazole based transporters

In a 50 mL round bottom flask, 2-chloro-1*H*-benzimidazole **7** (1 eq) was dissolved in 5mL EtOH. To this solution, corresponding anilines were added followed by the addition catalytic amount of HCl. This mixture was stirred at 103 °C for 12 hours. After reaction completion, the reaction mixture was dried in *vacuo*. The solid was dissolved in DCM and washed with water thrice. Then the organic layer was dried with brine solution followed by drying in Na$_2$SO$_4$.After drying, organic layer was evaporated in *vacuo*. The pure product was obtained by column chromatography (10% MeOH / CHCl$_3$) to yield yellowish to grey colored compound in 83-90% yield.

N-((*p*-bromo)phenyl)-1*H*-benzo[*d*]imidazol-2-amine 2a
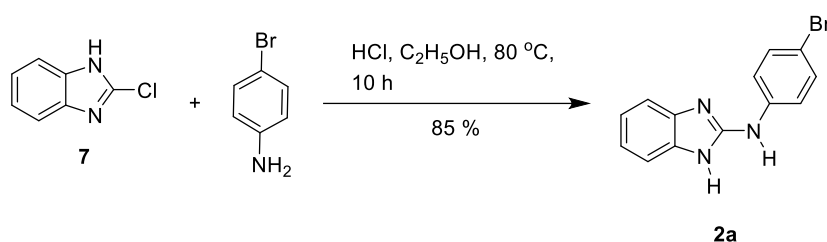


Yield: 85%.**^{1}H NMR (400 MHz, DMSO):** δ 10.98 (s, 1H), 9.58 (s, 1H), 7.76 (d, *J* = 8.0 Hz, 2H), 7.46 (d, *J* = 8.8 Hz, 2H), 7.32 (s, 2H), 6.99 (dd, *J* = 5.7, 3.1 Hz, 2H). **^{13}C NMR (101 MHz, CDCl$_3$):** δ 150.13, 140.33, 131.47, 120.26, 118.99, 111.69, 39.52.

**N-(4-(trifluoromethyl)phenyl)-1H-benzo[d]imidazol-2-amine 2b**
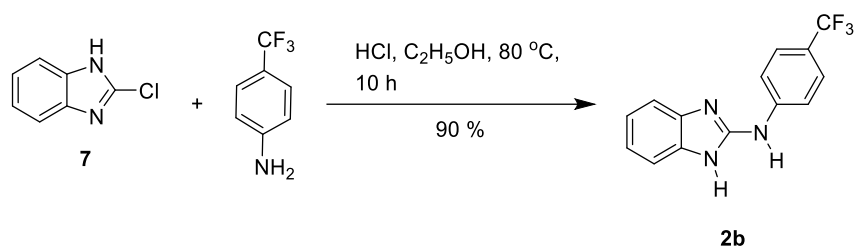
Yield: 90%. **^{1}H NMR (400 MHz, DMSO-D$_6$):** δ 11.13 (s, 1H), 9.93 (s, 1H), 7.97 (d, $J = $ 8.6 Hz, 2H), 7.66 (d, $J = $ 8.6 Hz, 2H), 7.36 (dd, $J = $ 32.1, 6.4 Hz, 2H), 7.08 – 6.99 (m, 2H). **^{13}C NMR (101 MHz, DMSO-D_6):** δ 149.63, 144.46, 142.69, 132.60, 126.16, 123.47, 120.45, 116.62, 109.73, 39.52.

N-(*p*-tolyl)-1H-benzo[d]imidazol-2-amine 2c
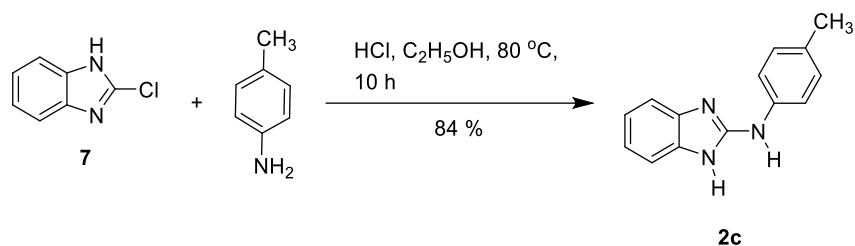
Yield: 84%. **^{1}H NMR (400 MHz, DMSO-D$_6$):** δ 11.17 (s, 1H), 9.42 (s, 1H), 7.61 (d, $J = $ 8.4 Hz, 2H), 7.30 (dd, $J = $ 5.8, 3.2 Hz, 2H), 7.13 (d, $J = $ 8.1 Hz, 2H), 6.99 (dd, $J = $ 5.8, 3.2 Hz, 2H), 2.26 (s, 3H).

N-(4-methoxyphenyl)-1H-benzo[d]imidazol-2-amine 2d
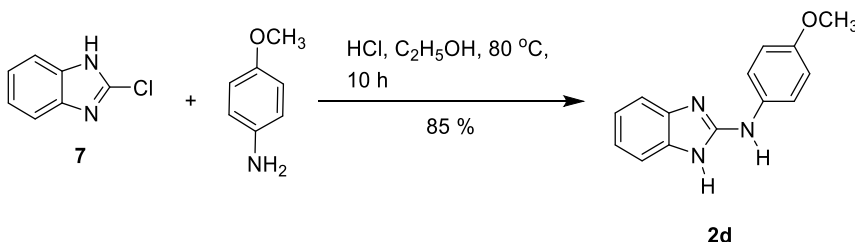
Yield: 85%. **^{1}H NMR (400 MHz, DMSO-d_6):** δ 10.79 (s, 1H), 9.15 (s, 1H), 7.69 – 7.58 (m, 2H), 7.26 (s, 2H), 6.99 – 6.92 (m, 2H), 6.93 – 6.88 (m, 2H), 3.73 (s, 3H). **^{13}C NMR (101 MHz, DMSO-D_6):** δ 153.70, 151.20, 134.22, 119.87, 118.80, 114.09, 85.61, 79.21, 55.23, 39.52.

Synthesis of benzimidazole based protransporter 1b

In a 50 mL round bottomed flask 2b (1 eq) was dissolved in acetone followed by the addition of *o*-nitro-bromobenzyl (1.5 eq). Catalytic amount of KOH was added to the reaction mixture. This reaction mixture was stirred for 10 hours at 80 °C. After the reaction completion, solvent was evaporated in *vacuo*. The solid was dissolved in DCM and washed 3 times with water. Then the organic layer was dried with brine followed by Na_2SO_4.Then the organic layer was dried in *vacuo* to get crude product, which was further purified, with column chromatography (10%MeOH/CHCl₃) to yield greenish white compound in 70% yield.
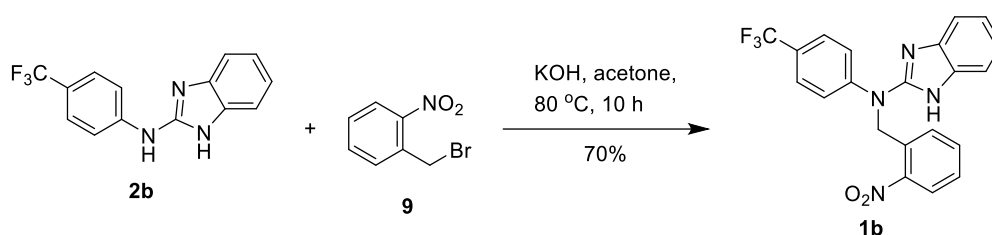
Yield : 70%.**¹H NMR (400 MHz, DMSO-*d₆*):** δ 9.42 (s, 1H), 8.26 (dd, *J* = 7.9, 1.6 Hz, 1H), 8.05 (d, *J* = 8.6 Hz, 2H), 7.66 (d, *J* = 8.7 Hz, 2H), 7.62 – 7.50 (m, 3H), 7.30 (d, *J* = 7.8 Hz, 1H), 7.09 (dtd, *J* = 42.3, 7.5, 1.1 Hz, 2H), 6.43 (dd, *J* = 7.7, 1.6 Hz, 1H), 5.95 (s, 2H).**¹³C NMR (101 MHz, DMSO):** δ 149.44, 147.25, 144.20, 141.49, 134.67, 133.45, 133.02, 128.57, 126.40, 125.94, 125.47, 121.71, 120.65, 117.59, 116.82, 109.00, 43.54, 39.52, 30.69.
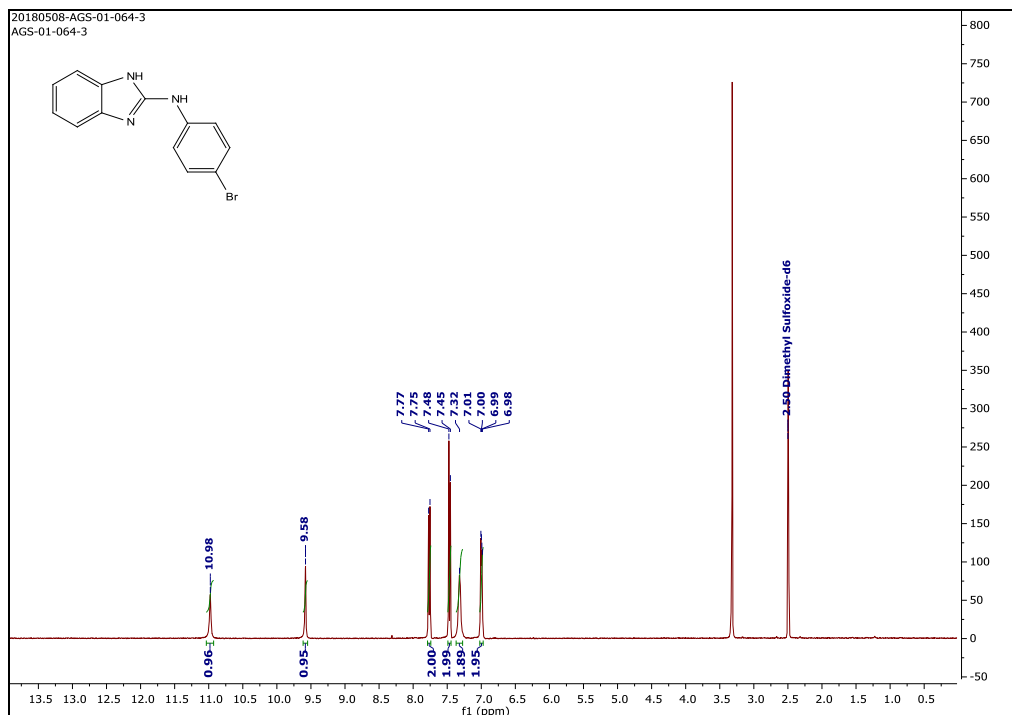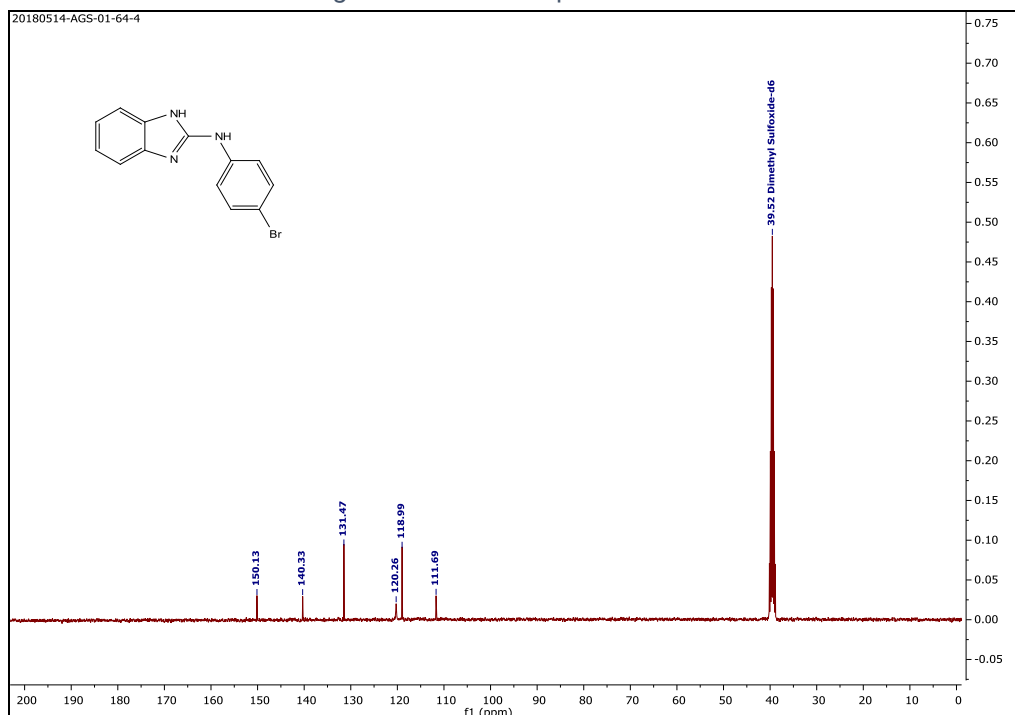
6. NMR data

Figure 24. ^{1}H NMR spectrum of **2a.**
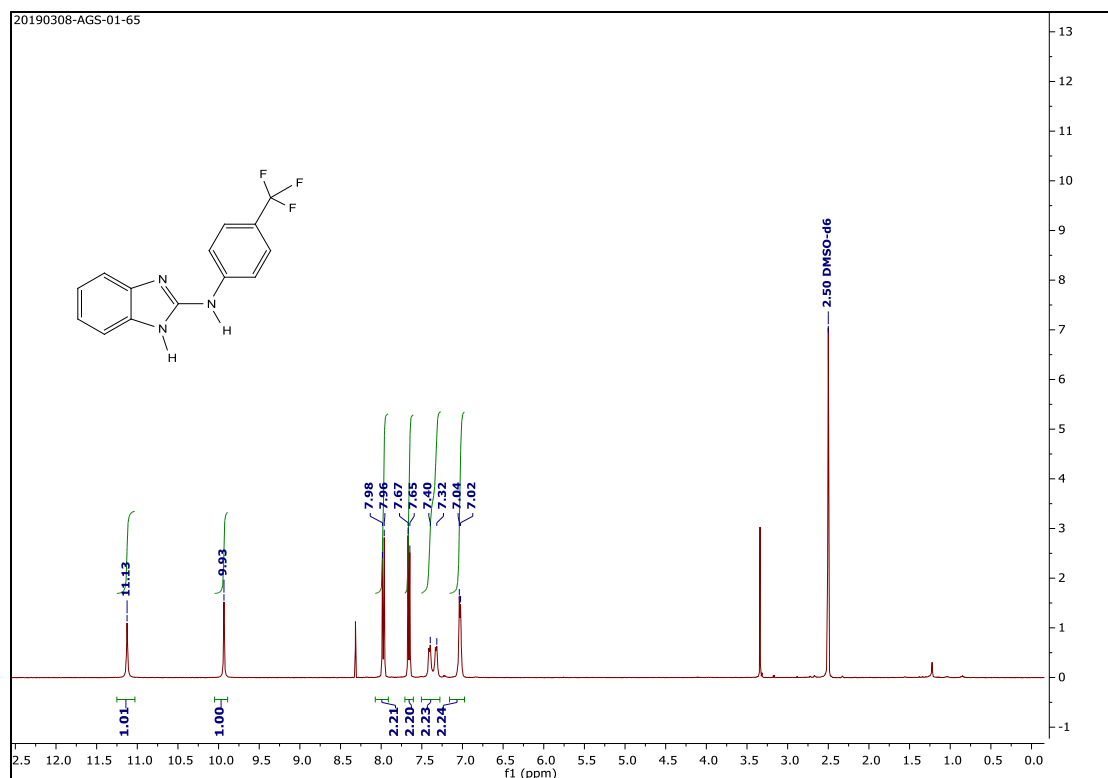

Figure 25. ^{13}C NMR spectrum of **2a**.

33

Figure 26. ^{1}H NMR spectrum of **2b**.
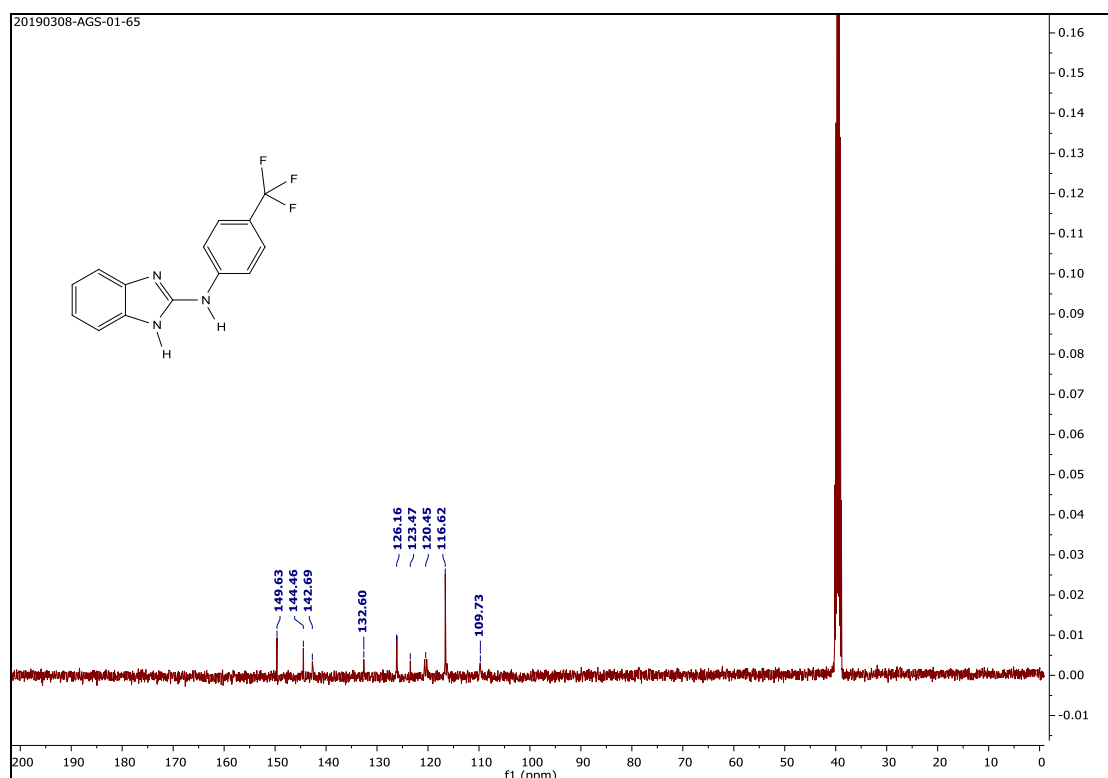
Figure 27. ^{13}C NMR spectrum of **2b**.
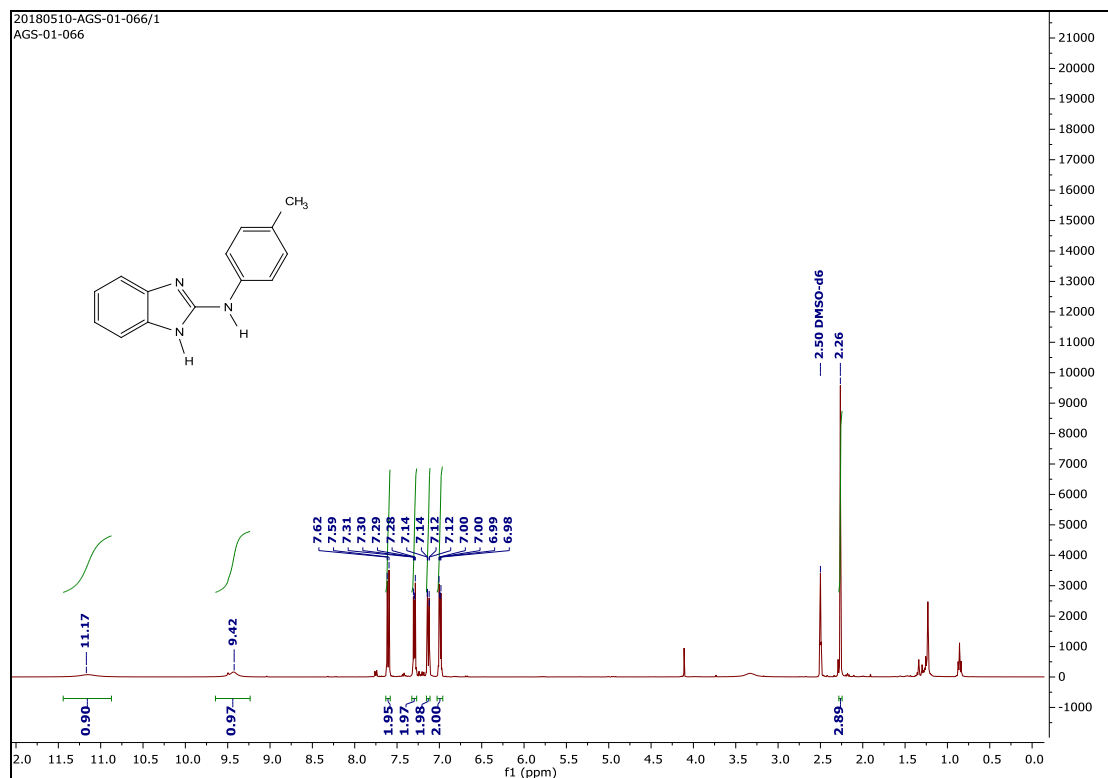
Figure 28. ^{1}H NMR spectrum of **2c**.
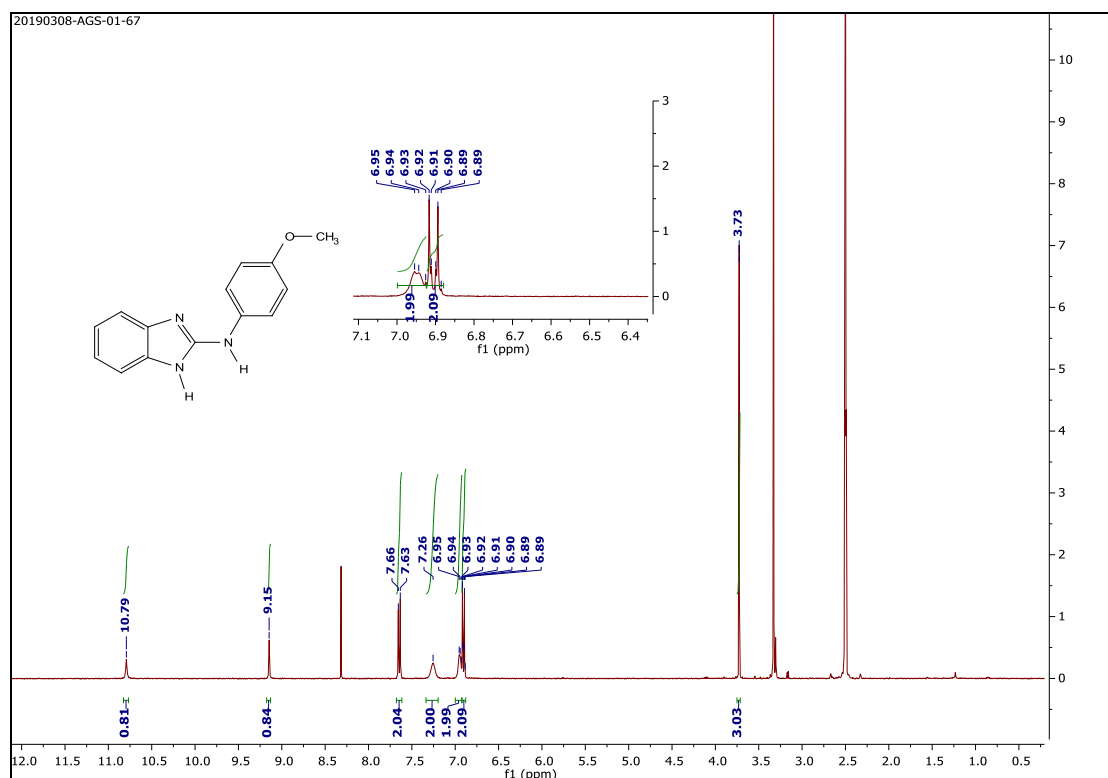
Figure 29. ¹H NMR spectrum of **2d**.

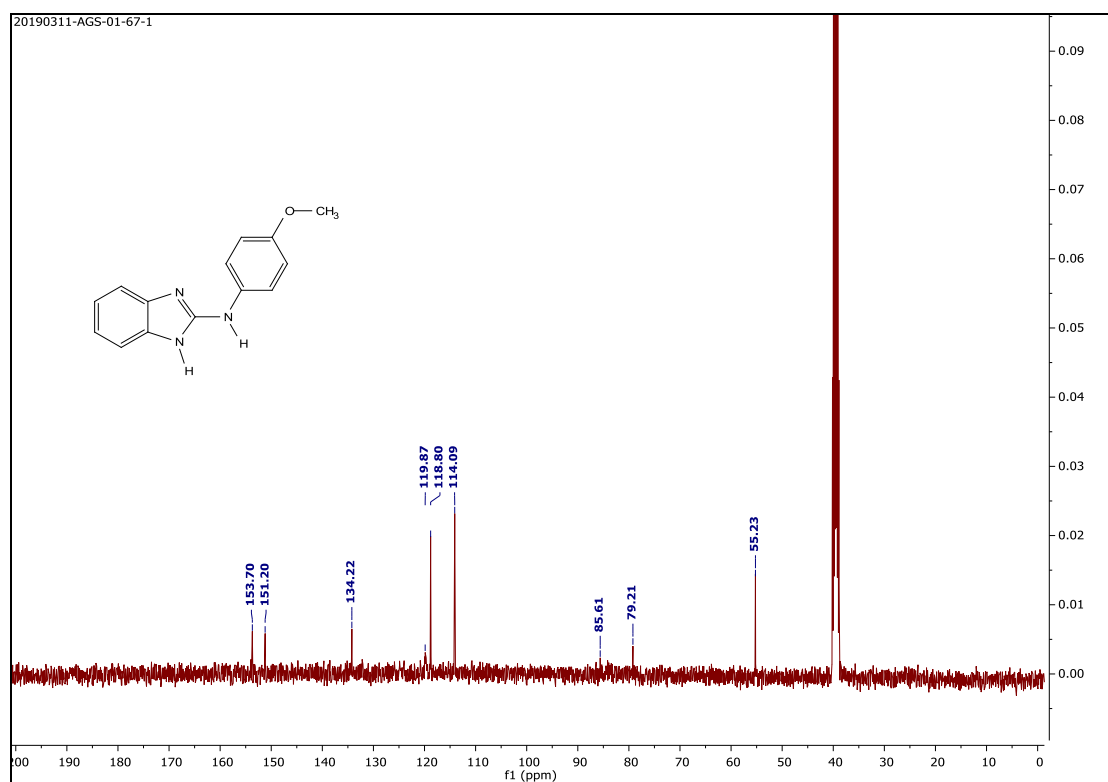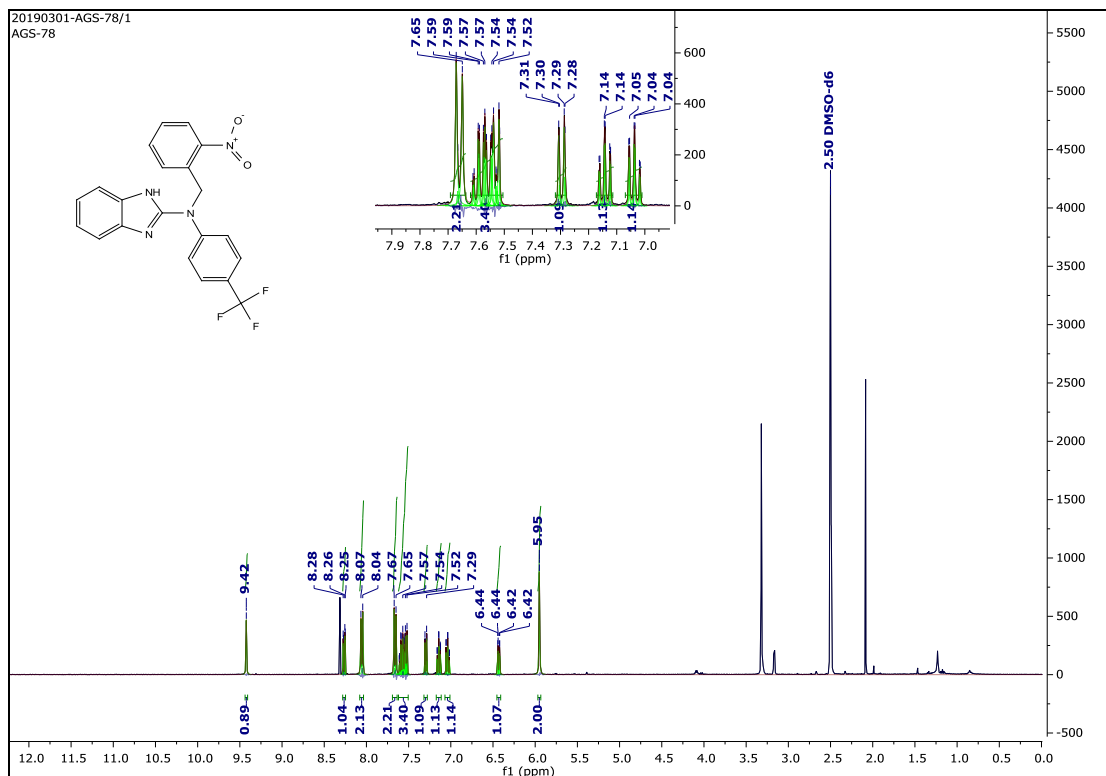*Figure 30.* ¹³C NMR spectrum of **2d**.

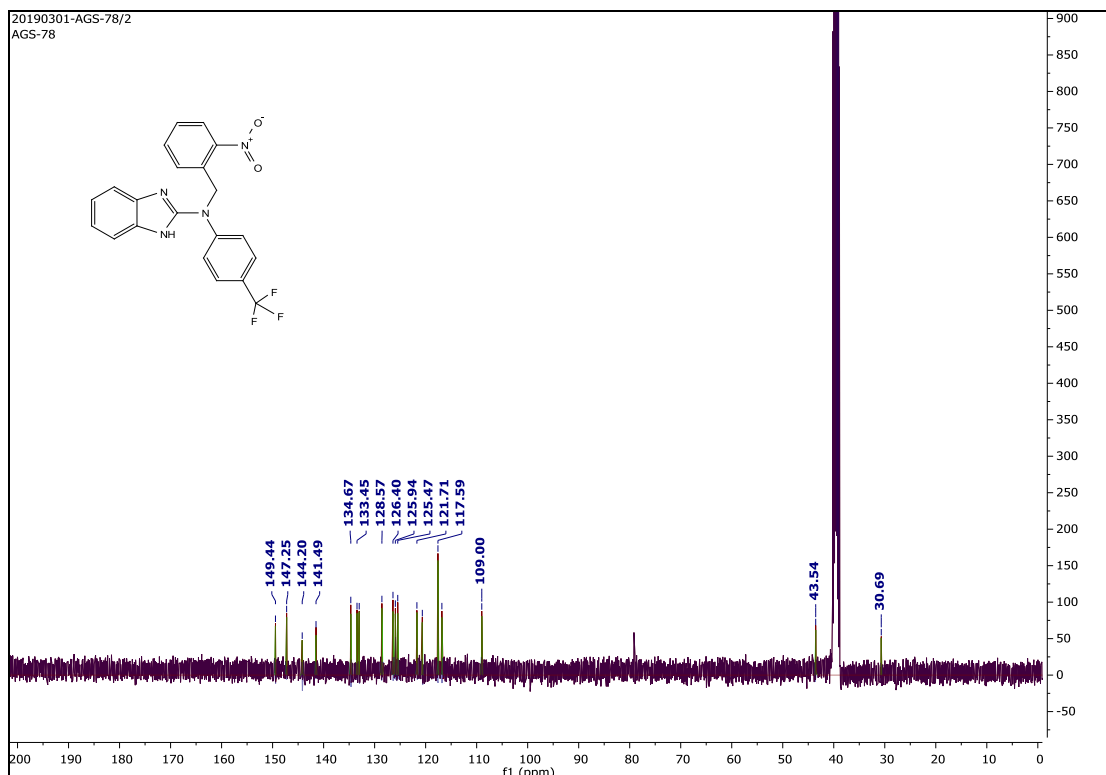*Figure 31.* ¹H NMR spectrum of **1b**.

Figure 32. ¹³C NMR spectrum of **1b**.

References:

(1)   Busschaert, N.; Wenzel, M.; Light, M. E.; Iglesias-Hernández, P.; Pérez-Tomás, R.; Gale, P. A. *J. Am. Chem. Soc.* **2011**, *133*, 14136–14148.

(2)   Davis, A. P.; Sheppard, D. N.; Smith, B. D. *Chem. Soc. Rev.* **2007**, *36*, 348–357.

(3)   Gale, P. A.; Davis, J. T.; Quesada, R. *Chem. Soc. Rev.* **2017**, *46*, 2497–2519.

(4)   Haynes, C. J. E.; Gale, P. A. *Chem. Commun.* **2011**, *47*, 8203–8209.

(5)   Santacroce, P. V.; Okunola, O. A.; Zavalij, P. Y.; Davis, J. T. *Chem. Commun.* **2006**, *0*, 3246–3248.

(6)   Lundberg, J. O.; Weitzberg, E.; Gladwin, M. T. *Nature Reviews Drug Discovery*. **2008**, 156–167.

(7)   Lundberg, J. O.; Weitzberg, E. *Nitric Oxide - Biology and Chemistry*. **2010**, 61–63.

(8)   Lundberg, J. O.; Gladwin, M. T.; Ahluwalia, A.; Benjamin, N.; Bryan, N. S.; Butler, A.; Cabrales, P.; Fago, A.; Feelisch, M.; Ford, P. C.; et al. In *Nature Chemical Biology*; **2009**; *5*, 865–869.

(9)   Mao, Y.; Yang, J.; Wang, Z.; Zhang, H.; Li, Z.; Struik, P. C.; Liu, L.; Gu, J. *Plant Sci.* **2018**, *274*, 320–331.

(10)   Dunkin, I. R.; Gębicki, J.; Kiszka, M.; Sanín-Leira, D. *J. Chem. Soc. Perkin Trans. 2* **2002**, *8*, 1414–1425.

(11)   Salunke, S. B.; Malla, J. A.; Talukdar, P. *Angew. Chemie Int. Ed.* **2019**, *58*, 5354–5358.

(12)   Marvin 5.8.0, ChemAxon, 2012 (http://www.chemaxon.com).

(13)   Biswas, S.; Bhattacharya, S. C.; Moulik, S. P. *J. Colloid Interface Sci.* **2004**; *271*, 157-162.

(14)   a) BindFit v0.5. http://app.supramolecular.org/bindfit/ (accessed June 2018); b) P. Thordarson, *Chem. Soc. Rev.* **2011**, *40*, 1305–1323.

(15)   Il'ichev, Y. V.; Schwörer, M. A.; Wirz, J. *J. Am. Chem. Soc.* **2004**, *126*, 4581–4595.

(16)   Kilchmann, F.; Marcaida, M. J.; Kotak, S.; Schick, T.; Boss, S. D.; Awale, M.; Gönczy, P.; Reymond, J. L. *J. Med. Chem.* **2016**, *59*, 7188–7211.